arXiv:1612.01729v1 [cond-mat.str-el] 6 Dec 2016

Anomalous violation of Fermi liquid theory in double- and triple-Weyl semimetals

Jing-Rong Wang,[1,2] Guo-Zhu Liu,[2,*] and Chang-Jin Zhang[1,3,†]

[1]*High Magnetic Field Laboratory, Hefei Institutes of Physical Science, Chinese Academy of Sciences, Hefei, Anhui 230031, P. R. China*

[2]*Department of Modern Physics, University of Science and Technology of China, Hefei, Anhui 230026, P. R. China*

[3]*Collaborative Innovation Center of Advanced Microstructures, Nanjing University, Nanjing 210093, P. R. China*

The influence of long-range Coulomb interaction on three-dimensional double- and triple-Weyl fermions is analyzed by means of renormalization group method after incorporating the dynamical screening effect caused by the collective particle-hole excitations. It is found that the quasiparticle residue Z_f of these two types of fermions vanishes in the lowest energy limit, indicating the violation of Fermi liquid description. Remarkably, Z_f flows to zero at low energies more slowly than a marginal Fermi liquid. Accordingly, the interaction-induced fermion damping effect is weaker than a marginal Fermi liquid. Therefore, the double- and triple-Weyl semimetals exhibit anomalous violation of the conventional Fermi liquid theory, which might be probed by such experimental apparatus as angle-resolved photoemission spectroscopy.

I. INTRODUCTION

In condensed matter physics, one fundamental issue is to determine whether the low-energy behavior of some correlated electron system can be described by the conventional Fermi liquid (FL) theory [1–3]. In a normal FL, the fermionic quasiparticles have a long lifetime and exhibit weak damping effect. To measure the strength of fermion damping, one needs to consider the fermion damping rate $\Gamma(\omega) \propto |\mathrm{Im}\Sigma^R(\omega)|$, where $\mathrm{Im}\Sigma^R(\omega)$ is the imaginary part of retarded fermion self-energy function. The fermions are expected to have a long lifetime if $\Gamma(\omega)$ vanishes more rapidly than ω as the Fermi surface is approached, namely

$$\lim_{\omega\to 0} \frac{\Gamma(\omega)}{\omega} \to 0. \tag{1}$$

In most cases, the fermion damping rate can be formally written as a power-law $\mathrm{Im}\Sigma^R(\omega) \propto |\omega|^x$. To judge whether FL theory works, one needs to compute the quasiparticle residue

$$Z_f(\omega) = \frac{1}{\left|1 - \frac{\partial}{\partial\omega}\mathrm{Re}\Sigma^R(\omega)\right|}, \tag{2}$$

where the real part of retarded fermion self-energy $\mathrm{Re}\Sigma^R(\omega)$ relates to $\mathrm{Im}\Sigma^R(\omega)$ via the Kramers-Kronig (KK) relationship. One can verify that Z_f takes certain finite value for $x > 1$, which implies that the FL theory is valid. In contrast, if $0 < x \leq 1$, the residue $Z_f = 0$, and we have a non-FL (NFL). The case of $x = 1$ represents a minimal violation of FL theory and thus defines a marginal Fermi liquid (MFL) [4], which is widely used to account for the observed unusual normal state of optimally doped high-T_c cuprate superconductors [3, 5, 6].

In a three-dimensional (3D) ordinary metal, the elementary fermionic excitations can be well described by the FL theory [1–3]. The validity of the FL description relies crucially on the fact that the long-range Coulomb interaction amongst fermions is screened by the collective particle-hole excitations and as such becomes short-ranged. Specifically, the bare Coulomb interaction behaves as $V(\mathbf{q}) \propto 1/q^2$ in 3D metals, but is modified by static screening to $V(\mathbf{q}) \propto 1/\left(q^2+\kappa\right)$, where the screening factor κ is determined by the zero-energy density of states (DOS) $\rho(0)$. Perturbative calculations [1, 2] show that the fermion damping rate depends on ω in the form $\mathrm{Im}\Sigma^R(\omega) \propto |\omega|^2$, which vanishes rapidly as $\omega \to 0$ and renders the applicability of conventional FL description.

Semimetals [7–11] are different from normal metals in that their Fermi surface shrinks to zero-dimensional points, at which the valence and conduction bands touch each other. The fermion DOS vanishes at the Fermi point, namely $\rho(0) = 0$, thus the Coulomb interaction remains long-ranged and might invalidate the FL description. This issue has been extensively studied in graphene by means of various techniques [12]. Earlier perturbative calculations found that the damping rate of Dirac fermions $\Gamma(\omega)$ displays a linear dependence on ω, which suggests a MFL behavior [13]. However, renormalization group (RG) calculations revealed a finite residue Z_f, so the fermions do have a quasiparticle peak in their spectral function [14, 15].

Owing to the intriguing properties and potential applications, 3D Weyl semimetal [16–18] has been extensively studied in recent years. In a Weyl semimetal, the fermions display a linear dispersion around pairs of Weyl points with monopole charge ± 1. Experimentally, Weyl semimetallic state has been observed in TaAs [19–22], NbAs [23], TaP [24, 25], and NbP [26, 27] by angle-resolved photoemission spectroscopy (ARPES) measurements. Moreover, first-principle calculations predicted that an ideal Weyl semimetal with only symmetry-related Weyl points may be realized in such materials as $CuTlSe_2$, $AgTlTe_2$, $AuTlTe_2$, and $ZnPbAs_2$ *etc.* [28, 29].

*Corresponding author: gzliu@ustc.edu.cn

†Corresponding author: zhangcj@hmfl.ac.cn

Material	Fermion dispersion	Z_f	Damping rate	Reference
2D Dirac SM	$E=\pm v\lvert\mathbf{k}\rvert$	$Z_f\to$ Const.	$\mathrm{Im}\Sigma^R(\omega)=\omega^2/\ln^2(\omega_0/\omega)$	[14]
2D Semi-Dirac SM	$E=\pm\sqrt{A^2k_x^4+v^2k_y^2}$	$Z_f\to 0$	$\mathrm{Im}\Sigma^R(\omega)\sim\omega\left[\ln(\omega_0/\omega)\right]^{\eta_A}$	[61]
3D Dirac/Weyl SM	$E=\pm v\lvert\mathbf{k}\rvert$	$Z_f\to$ Const.	-	[74]
3D ani-Weyl SM	$E=\pm\sqrt{v^2k_\perp^2+A^2k_z^4}$	$Z_f\to$ Const.	-	[76, 77]
3D quadratic SM	$E=\pm A\lvert\mathbf{k}\rvert^2$	$Z_f\to 0$	$\mathrm{Im}\Sigma^R(\omega)\sim\omega^{1-\eta_B}$	[78–80]
3D nodal line SM	$E=\pm\sqrt{A^2(k_\perp^2-k_F^2)^2+v^2k_z^2}$	$Z_f\to$ Const.	$\mathrm{Im}\Sigma^R(\omega)\sim\omega^2$	[86]
3D double-Weyl SM	$E=\pm\sqrt{A^2k_\perp^4+v^2k_z^2}$	$Z_f\to 0$	$\mathrm{Im}\Sigma^R(\omega)\sim\omega/\left[\ln(\omega_0/\omega)\right]^{\eta_C}$	
3D triple-Weyl SM	$E=\pm\sqrt{B^2k_\perp^6+v^2k_z^2}$	$Z_f\to 0$	$\mathrm{Im}\Sigma^R(\omega)\sim\omega/\left[\ln(\omega_0/\omega)\right]^{\eta_D}$	

TABLE I: Residue Z_f and fermion damping rate in various semimetals. Here, η_A, η_B, η_C, and η_D are all positive constants.

Apart from the usual Weyl semimetals, double- and triple-Weyl semimetals, in which the monopole charges of the Weyl points are ±2 and ±3 respectively, also have attracted considerable interest [30–58]. The dispersion of double- (triple-) Weyl fermions are linear in one component of the momenta, but exhibits quadratic (cubic) dependence on the rest two components.

In this paper, we show that the conventional FL theory is violated in a new manner in double- and triple-Weyl semimetals. In particular, although the fermion damping rate satisfies the condition $\lim_{\omega\to0}\frac{\Gamma(\omega)}{\omega}\to0$, the residue Z_f vanishes in the lowest energy limit. It therefore turns out that double- and triple-Weyl semimetals exhibit a smaller deviation of the FL theory than MFL. To illustrate the existence of such an anomalous violation of FL theory, we shall compute the damping rate $\Gamma(\omega)$ and the residue Z_f of both double- and triple-Weyl fermions by performing a detailed RG analysis of the effects of long-range Coulomb interaction [59, 60].

We notice that the physical effects of long-range Coulomb interaction on double- and triple-Weyl fermions have recently been studied theoretically [40–42]. It was found that Coulomb interaction is marginally irrelevant in double- and triple-Weyl semimetals. These works are technically based on the instantaneous approximation for the Coulomb interaction. We emphasize that, in order to precisely compute Z_f and fermion damping rate, the dynamical screening needs to be properly taken into account. Moreover, the validity of FL theory cannot be simply determined by the marginal irrelevance of Coulomb interaction. Even a marginally irrelevant Coulomb interaction is able to induce nontrivial low-energy properties. For instance, the Coulomb interaction is known to be marginally irrelevant in both 2D Dirac semimetal [14, 15] and 2D semi-Dirac semimetal [61, 62]. However, it has distinct physical effects in these two materials: Z_f flows to a finite value at low energies in the former material, but vanishes in the latter. Apparently, the fermion dispersion plays a vital role, and a more careful theoretical investigation is necessary.

Concerning the methodology, ordinary perturbative expansion method is not a suitable tool to compute the fermion damping rate and residue. RG method is more appropriate since it naturally produces the energy dependence of all the model parameters. In this paper, we shall make use of the RG approach in combination with $1/N$ expansion, where N is the fermion flavor. To get a quantitatively more precise fermion self-energy, we go beyond the instantaneous approximation and incorporate the energy dependence of Coulomb interaction by including the dynamical polarization function. We shall derive the RG equations for all the model parameters, and then extract some useful physical quantities from the solutions of RG equations. Our main conclusion is that the FL theory breaks down in both double- and triple-Weyl semimetals as the residue $Z_f\to0$ in the lowest energy limit. Nevertheless, Z_f flows to zero more slowly than a logarithmic decay, signalling a smaller-than-MFL deviation of the conventional FL description.

On the experimental side, our RG analysis would shed light on the exploration of anomalous violation of FL theory in some real materials. It has been suggested that $HgCr_2Se_4$ [31] and $SrSi_2$ [35] are two potential examples of double-Weyl semimetals. Recent transport measurements reported strong evidence of the half-metallicity of $HgCr_2Se_4$ [36]. Theoretical studies proposed that cubic Dirac semimetal might be realized in some candidates, including $Rb(MoTe)_3$ and $Tl(MoTe)_3$ of the $A(MoX)_3$ family [37]. Moreover, double- and triple-Weyl fermions can be realized by microwave experiments [38, 39]. We expect that ARPES is an efficient apparatus to detect the strange non-FL state in some of these materials.

In Table I, we present a summary of the low-energy asymptotic behaviors of the residue Z_f and the fermion damping rate $\mathrm{Im}\Sigma^R(\omega)$ obtained in various semimetals. A clear indication is that the nature of strict ground state and the low-energy physics depend crucially on the spatial dimension and fermion dispersion of the material.

The rest of the paper will be organized as follows. We present the model Hamiltonian in Sec. II. In Sec. III, we derive the RG equations for the model parameters of double- and triple-Weyl fermions, respectively. The numerical solutions of RG equations are analyzed in Sec. IV. In Sec. V, we make a comparison between different RG schemes. We summarize the main results in Sec. VI. All the computational details are given in Appendixes A-E.

II. MODEL HAMILTONIAN

The Hamiltonian for the free double-Weyl fermions has the form [40, 41, 43]

$$H_d = \sum_{a=1}^{N}\int d^3\mathbf{x}\psi^{\dagger}_{d,a}(\mathbf{x})\left[-A\left(\partial_x^2-\partial_y^2\right)\sigma_x -2A\partial_x\partial_y\sigma_y - iv\partial_z\sigma_z\right]\psi_{d,a}(\mathbf{x}), \quad (3)$$

and the Hamiltonian for the free triple-Weyl fermions is written as [42]

$$H_t = \sum_{a=1}^{N}\int d^3\mathbf{x}\psi_{d,a}\dagger(\mathbf{x})\left[iB\left(\partial_x^3-\partial_x\partial_y^2\right)\sigma_x +iB\left(\partial_y^3-\partial_y\partial_x^2\right)\sigma_y - iv\partial_z\sigma_z\right]\psi_{d,a}(\mathbf{x}). \quad (4)$$

Here, we use $\psi_{d,a}$ and $\psi_{t,a}$ to represent the two-component spinor fields for double- and triple-Weyl fermions, respectively. The flavor index a is $a = 1, 2, 3, ..., N$ with N being the number of fermion flavor, and $\sigma_{x,y,z}$ are the standard Pauli matrices. There are two model parameters A and v introduced to characterize the spectrum of double-Weyl fermions, satisfying $E_d = \sqrt{A^2k_\perp^4+v^2k_z^2}$. The dispersion of triple-Weyl fermions is defined as $E_t = \sqrt{B^2k_\perp^6+v^2k_z^2}$ through two parameters B and v. These fermions are subject to the long-range Coulomb interaction, described by

$$H_{\rm C} = \frac{1}{4\pi}\sum_{a=1}^{N}\int d^3\mathbf{x}d^3\mathbf{x}'\rho_a(\mathbf{x})\frac{e^2}{\epsilon\left|\mathbf{x}-\mathbf{x}'\right|}\rho_a^{\dagger}(\mathbf{x}'), \quad (5)$$

where the fermion density operator is given by

$$\rho_a(\mathbf{x}) = \psi_a^{\dagger}(\mathbf{x})\psi_a(\mathbf{x}).$$

The total model will be treated by making perturbative expansion in powers of $1/N$ with N being a large general number.

The free propagator of double-Weyl fermions reads

$$G_{d,0}(\omega,\mathbf{k}) = \frac{1}{i\omega-\left(Ad_1(\mathbf{k})\sigma_x+Ad_2(\mathbf{k})\sigma_y+vk_z\sigma_z\right)}, \quad (6)$$

where $d_1(\mathbf{k}) = \left(k_x^2-k_y^2\right)$ and $d_2(\mathbf{k}) = 2k_xk_y$. The free propagator of triple-Weyl fermions is

$$G_{t,0}(\omega,\mathbf{k}) = \frac{1}{i\omega-\left(Bg_1(\mathbf{k})\sigma_x+Bg_2(\mathbf{k})\sigma_y+vk_z\sigma_z\right)}, \quad (7)$$

where $g_1(\mathbf{k}) = \left(k_x^3-3k_xk_y^2\right)$ and $g_2(\mathbf{k}) = \left(k_y^3-3k_yk_x^2\right)$. Independent of the fermion dispersion, the bare Coulomb interaction function takes the form in momentum space:

$$V_0(\mathbf{q}) = \frac{4\pi e^2}{\epsilon|\mathbf{q}|^2} = \frac{4\pi\alpha v}{|\mathbf{q}|^2}, \quad (8)$$

where $\alpha = e^2/\epsilon v$ serves as an effective interaction strength, with e being the electron charge and ϵ dielectric constant. After including the dynamical screening caused by the polarization function, one can write the dressed Coulomb interaction function as

$$V_{d,t}(\Omega,\mathbf{q}) = \frac{1}{V_0^{-1}(\mathbf{q})+\Pi_{d,s}(\Omega,\mathbf{q})}, \quad (9)$$

in which the polarization function for double- and triple-Weyl fermions are defined as

$$\Pi_d(\Omega,\mathbf{q}) = -N\int\frac{d\omega}{2\pi}\frac{d^3\mathbf{k}}{(2\pi)^3}\mathrm{Tr}\left[G_{d0}(\omega,\mathbf{k})\times G_{d0}(\omega+\Omega,\mathbf{k}+\mathbf{q})\right] \quad (10)$$

and

$$\Pi_t(\Omega,\mathbf{q}) = -N\int\frac{d\omega}{2\pi}\frac{d^3\mathbf{k}}{(2\pi)^3}\mathrm{Tr}\left[G_{t0}(\omega,\mathbf{k})\times G_{t0}(\omega+\Omega,\mathbf{k}+\mathbf{q})\right], \quad (11)$$

to the leading order of $1/N$ expansion. It is technically troublesome to obtain a complete analytical expression of $\Pi_d(\Omega,\mathbf{q})$ or $\Pi_t(\Omega,\mathbf{q})$. According to the calculations presented in Appendix A, Π_d can be approximated by

$$\Pi_d(\Omega,\mathbf{q}) \approx N\left[\frac{q_\perp^2}{3\pi^2v}\ln\left(\frac{\sqrt{A}\Lambda_{UV}+\left(\Omega^2+A^2q_\perp^4\right)^{\frac{1}{4}}}{\left(\Omega^2+A^2q_\perp^4\right)^{\frac{1}{4}}}\right)+\frac{1}{64A}\frac{vq_z^2}{\sqrt{\Omega^2+v^2q_z^2}}\right]. \quad (12)$$

As shown in Appendix C, one can simplify the expression of Π_t in the form

$$\Pi_t(\Omega,\mathbf{q}) \approx N\left[\frac{3q_\perp^2}{4\pi^2v}\ln\left(\frac{B^{\frac{1}{3}}\Lambda_{UV}+\left(\Omega^2+B^2q_\perp^6\right)^{\frac{1}{6}}}{\left(\Omega^2+B^2q_\perp^6\right)^{\frac{1}{6}}}\right)+c_t\frac{1}{B^{\frac{2}{3}}}\frac{vq_z^2}{\left(\Omega^2+v^2q_z^2\right)^{\frac{2}{3}}}\right], \quad (13)$$

where

$$c_t = \frac{2^{\frac{1}{3}}\pi^{\frac{1}{2}}}{90\Gamma\left(\frac{5}{6}\right)\Gamma\left(\frac{2}{3}\right)} \approx 0.0162333. \quad (14)$$

III. DERIVATION OF RG EQUATIONS

The influence of long-range Coulomb interaction has been extensively investigated in the contexts of a large number of semimetals [12, 14, 15, 40–42, 61–88]. The calculations based on modern RG theory revealed that Coulomb interaction plays quite different roles in various semimetals. In 2D Dirac semimetal [12, 14, 15, 64–66, 69, 70], 2D semi-Dirac semimetal [61, 87], 3D Dirac/Weyl semimetal [71–73, 75], 3D double-Weyl semimetal [40, 41], and 3D triple-Weyl semimetal [42], the effective strength of Coulomb interaction was found to vanish in the lowest energy limit, but at a low speed, which

indicates that Coulomb interaction is marginally irrelevant in these semimetals. However, this does not mean that Coulomb interaction can be neglected. Indeed, the marginally irrelevant Coulomb interaction leads to unusual renormalization of fermion velocity, which increases to larger values as the energy scale is lowered [14, 15, 40–42, 61, 63–66, 71, 72, 75, 87]. Accordingly, a number of observable quantities, such as specific heat, compressibility, and optical conductivity *etc.*, acquire logarithmic-like corrections [40–42, 61, 67, 68, 71, 72, 87]. The renoramalized fermion velocity has already been observed in ultra clean suspended graphene [89], quasi-freestanding graphene on silicon carbide (SiC) [90], and graphene on boron nitride substrate [91]. The observed renormalization of fermion dispersion in topological insulator-like system of Bi bilayer grown on Bi_2Se_3 [92] is also expected to be caused by Coulomb interaction. For a 3D quadratic semimetal, RG studies showed that Coulomb interaction is relevant and produce non-FL behaviors [80]. Recent experiment based on ARPES method provided some evidence of NFL state in $Pr_2Ir_2O_7$ [93]. It also has been found that the effective strength of Coulomb interaction flows to zero exponentially at low energies in a 3D anisotropic Weyl (ani-Weyl) semimetal [76] and in a nodal-line semimetal [86]. Since Coulomb interaction is irrelevant, the observable quantities exhibit qualitatively the same behaviors as a free fermion system [76].

In many cases, RG approach is a more powerful tool than ordinary perturbative expansion method in the determination of damping rate and Z_f [14, 15, 61]. As mentioned in Sec. I, direct perturbative calculations found a MFL behavior of Dirac fermions in graphene with a vanishing Z_f [13]. However, more careful RG studies discovered that Z_f actually flows to a finite value [14, 15], which means the ordinary FL theory is valid. In the following, we shall make use of the RG method to carefully analyze the asymptotic behavior of Z_f and damping rate.

In this section, we evaluate the fermion self-energy and then derive the RG equations for all the model parameters. The evaluation will be performed first in the case of double-Weyl semimetal and then triple-Weyl semimetal.

A. Double-Weyl semimetal

The self-energy of double-Weyl fermions induced by the long-range Coulomb interaction is given by

$$\Sigma_d(\omega,\mathbf{k}) = \int' \frac{d\Omega}{2\pi}\frac{d^3\mathbf{q}}{(2\pi)^3} G_{d0}(\omega+\Omega,\mathbf{k}+\mathbf{q})V_d(\Omega,\mathbf{q}), \tag{15}$$

where integration $\int' \frac{d\Omega}{2\pi}\frac{d^3\mathbf{q}}{(2\pi)^3}$ denotes a specifically chosen momentum shell. Firstly, we employ the RG scheme

$$-\infty<\Omega<\infty, \qquad b\Lambda<E_d<\Lambda, \tag{16}$$

where $E_d=\sqrt{A^2q_\perp^4+v^2q_z^2}$ and $b=e^{-l}$ with l being a varying length scale. After carrying out detailed computations, which are given in Appendix B, we find that $\Sigma_d(\omega,\mathbf{k})$ can be approximated as

$$\begin{aligned}\Sigma_d(\omega,\mathbf{k}) &\approx [i\omega C_{d1} - [Ad_1(\mathbf{k})\sigma_x + Ad_2(\mathbf{k})\sigma_y]\, C_{d2} \\ &\quad -vk_z\sigma_z C_{d3}]\ln(b^{-1}).\end{aligned} \tag{17}$$

The expressions of parameters $C_{d,i}$ with $i=1,2,3$ are shown in Appendix B. We can formally write these parameters as $C_{d,i}\equiv C_{d,i}(\alpha,\beta_d,\gamma_d)$ with

$$\beta_d=\frac{A\Lambda}{v^2}, \quad \gamma_d=\frac{\sqrt{A}\Lambda_{UV}}{\sqrt{\Lambda}}. \tag{18}$$

To proceed, we rewrite the free action of double-Weyl fermions as

$$\begin{aligned}S^0_{\psi_d} &= \int \frac{d\omega}{2\pi}\frac{d^3\mathbf{k}}{(2\pi)}\psi_d^\dagger(\omega,\mathbf{k})\,(i\omega - Ad_1(\mathbf{k})\sigma_x - Ad_2(\mathbf{k})\sigma_y \\ &\quad -vk_z\sigma_z)\,\psi_d(\omega,\mathbf{k}).\end{aligned} \tag{19}$$

Including the fermion self-energy induced by Coulomb interaction, the above action becomes

$$\begin{aligned}S_{\psi_d} &= \int \frac{d\omega}{2\pi}\frac{d^3\mathbf{k}}{(2\pi)}\psi_d^\dagger(\omega,\mathbf{k})\,(i\omega - Ad_1(\mathbf{k})\sigma_x - Ad_2(\mathbf{k})\sigma_y \\ &\quad -vk_z\sigma_z + \Sigma_d(\omega,\mathbf{k}))\,\psi_d(\omega,\mathbf{k}) \qquad (20)\\ &\approx \int \frac{d\omega}{2\pi}\frac{d\mathbf{k}}{(2\pi)}\psi_d^\dagger(\omega,\mathbf{k})\,\big[i\omega e^{C_{d1}l} - (Ad_1(\mathbf{k})\sigma_x \\ &\quad +Ad_2(\mathbf{k})\sigma_y)\,e^{C_{d2}l} - vk_z\sigma_z e^{C_{d3}l}\big]\,\psi_d(\omega,\mathbf{k}). \qquad (21)\end{aligned}$$

We then make the following scaling transformations

$$\begin{aligned}k_x &= k_x' e^{-\frac{l}{2}}, &(22)\\ k_y &= k_y' e^{-\frac{l}{2}}, &(23)\\ k_z &= k_z' e^{-l}, &(24)\\ \omega &= \omega' e^{-l}, &(25)\\ \psi &= \psi' e^{\left(2-\frac{C_{d1}}{2}\right)l}, &(26)\\ A &= A' e^{(C_{d1}-C_{d2})l}, &(27)\\ v &= v' e^{(C_{d1}-C_{d3})l}, &(28)\end{aligned}$$

which leads us to

$$\begin{aligned}S_{\psi_d'} &= \int \frac{d\omega'}{2\pi}\frac{d^3\mathbf{k}'}{(2\pi)^3}\psi_d'^\dagger(\omega',\mathbf{k}')\,(i\omega' - A'd_1(\mathbf{k}')\sigma_x \\ &\quad -A'd_2(\mathbf{k}')\sigma_y - v'k_z'\sigma_z)\,\psi_d'(\omega',\mathbf{k}').\end{aligned} \tag{29}$$

This action has the same form as the free action, which enables us to derive the flow equations.

From Eq. (26), the RG equation for the residue is found to have the form

$$\frac{dZ_f}{dl} = -C_{d1}Z_f. \tag{30}$$

According to Eqs. (27) and (28), we find that the RG equations of A and v are

$$\begin{aligned}\frac{dA}{dl} &= (C_{d2}-C_{d1})\,A, &(31)\\ \frac{dv}{dl} &= (C_{d3}-C_{d1})\,v. &(32)\end{aligned}$$

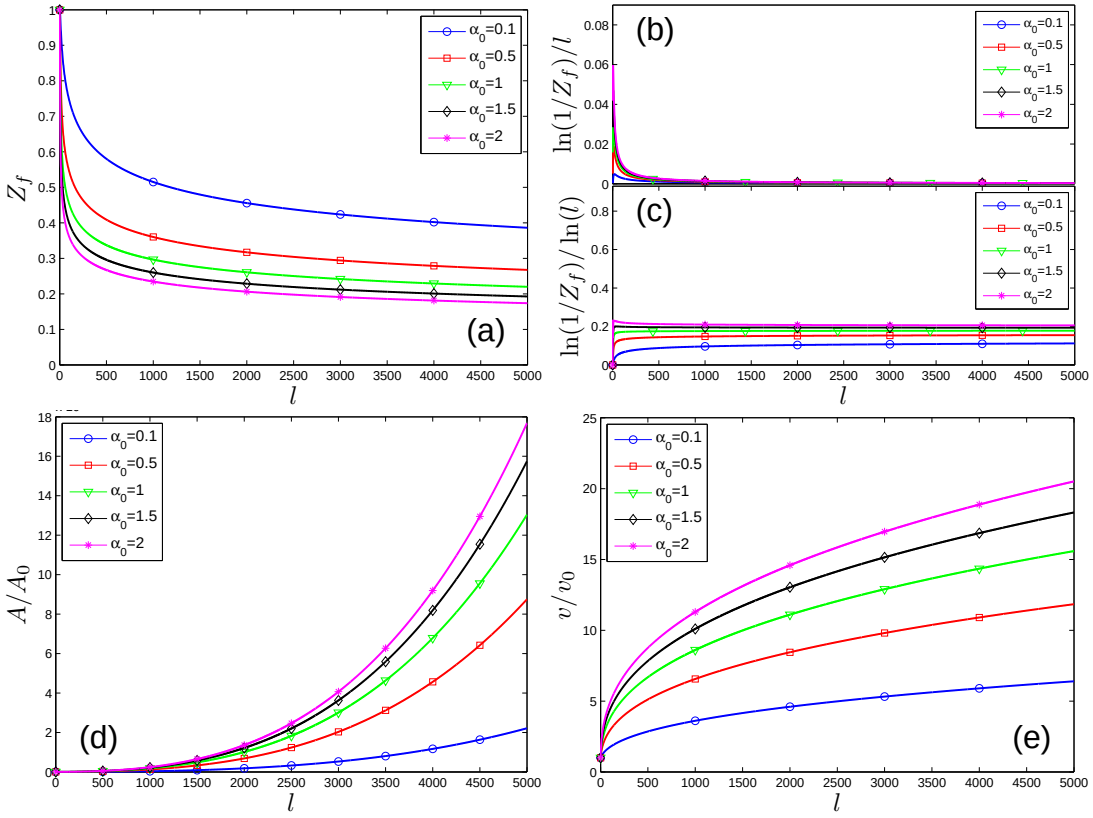

FIG. 1: Flow of Z_f, A, and v in double-Weyl semimetal at different values of α_0. $N = 2$, $\beta_{d0} = 1$, and $\gamma_{d0} = 0.2$.

The RG equations of other parameters α, β_d, and γ are

$$\frac{d\alpha}{dl} = (C_{d1} - C_{d3})\,\alpha, \tag{33}$$

$$\frac{d\beta_d}{dl} = (C_{d1} + C_{d2} - 2C_{d3} - 1)\,\beta_d, \tag{34}$$

$$\frac{d\gamma_d}{dl} = \frac{1}{2}(C_{d2} - C_{d1} + 1)\gamma_d. \tag{35}$$

B. Triple-Weyl semimetal

The Coulomb interaction gives rise to the following self-energy of triple-Weyl fermions:

$$\Sigma_t(\omega, \mathbf{k}) = \int' \frac{d\Omega}{2\pi}\frac{d^3\mathbf{q}}{(2\pi)^3} G_{t0}(\omega + \Omega, \mathbf{k} + \mathbf{q}) V_t(\Omega, \mathbf{q}), \tag{36}$$

which will be calculated by adopting the RG scheme

$$-\infty < \Omega < \infty, \qquad b\Lambda < E_t < \Lambda, \tag{37}$$

where $E_t = \sqrt{B^3 q_\perp^6 + v^2 q_z^2}$. We know from Appendix D that

$$\Sigma_t(\omega, \mathbf{k}) \approx [i\omega C_{t1} - (Bg_1(\mathbf{k})\sigma_x + Bg_2(\mathbf{k})\sigma_y)\, C_{t2} - vk_z\sigma_z C_{t3}] \ln(b^{-1}), \tag{38}$$

where $C_{t,i} \equiv C_{t,i}(\alpha, \beta_t, \gamma_t)$ with

$$\beta_t = \frac{B^{\frac{2}{3}}\Lambda^{\frac{4}{3}}}{v^2}, \quad \gamma_t = \frac{B^{\frac{1}{3}}\Lambda_{UV}}{\Lambda^{\frac{1}{3}}}. \tag{39}$$

The detailed expressions of $C_{t,i}$ are given in Appendix D.

By repeating the same computational procedure adopted in the case of double-Weyl semimetal, we add the self-energy to free action and then obtain

$$S_{\psi_t} = \int \frac{d\omega}{2\pi}\frac{d^3\mathbf{k}}{(2\pi)^3}\psi_t^\dagger(\omega, \mathbf{k}) \left[i\omega e^{C_{t1}l} - (Bg_1(\mathbf{k})\sigma_x + Bg_2(\mathbf{k})\sigma_y)\, e^{C_{t2}l} - vk_z\sigma_z e^{C_{t3}l}\right] \psi_t(\omega, \mathbf{k}). \tag{40}$$

Making use of the scaling transformations

$$k_x = k_x' e^{-\frac{l}{3}}, \tag{41}$$

$$k_y = k_y' e^{-\frac{l}{3}}, \tag{42}$$

$$k_z = k_z' e^{-l}, \tag{43}$$

$$\omega = \omega' e^{-l}, \tag{44}$$

$$\psi_t = \psi_t' e^{(\frac{11}{6} - \frac{C_{t1}}{2})l}, \tag{45}$$

$$B = B' e^{(C_{t1} - C_{t2})l}, \tag{46}$$

$$v = v' e^{(C_{t1} - C_{t3})l}, \tag{47}$$

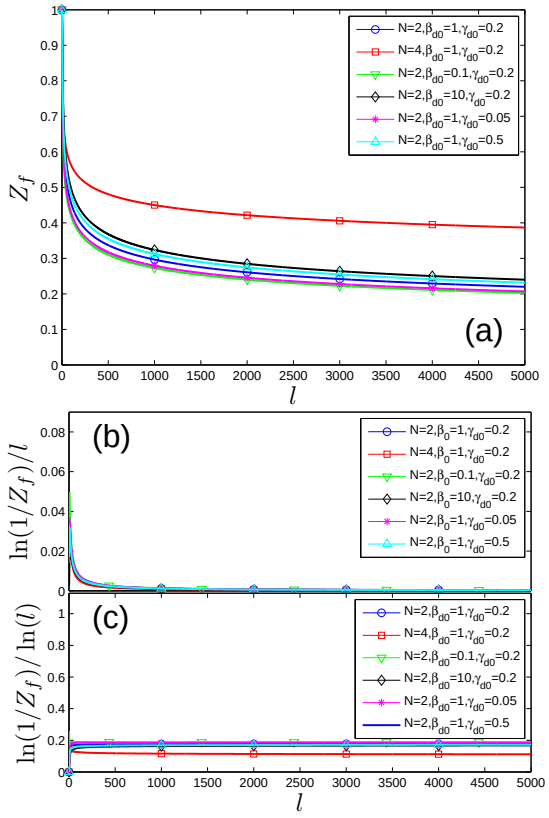

FIG. 2: Flow of Z_f in double-Weyl semimetal at different values of N, β_{d0}, and γ_{d0}. Here, $\alpha_0 = 1$.

the above action is converted to

$$S_{\psi'_t} = \int \frac{d\omega'}{2\pi}\frac{d^3\mathbf{k}'}{(2\pi)^3}\psi'^{\dagger}_t(\omega',\mathbf{k}')\left[i\omega' - (B'g_1(\mathbf{k}')\sigma_x + B'g_2(\mathbf{k}')\sigma_y) - v'k'_z\sigma_z\right]\psi'_t(\omega',\mathbf{k}'), \quad (48)$$

which recovers the same form as the free action. From the transformations (45)-(47), we get the RG equations for Z_f, B, and v

$$\frac{dZ_f}{dl} = -C_{t1}Z_f, \quad (49)$$

$$\frac{dB}{dl} = (C_{t2} - C_{t1})B, \quad (50)$$

$$\frac{dv}{dl} = (C_{t3} - C_{t1})v. \quad (51)$$

The RG equations of α, β_t, and γ_t are given by

$$\frac{d\alpha}{dl} = (C_{t1} - C_{t3})\,\alpha, \quad (52)$$

$$\frac{d\beta_t}{dl} = \left(\frac{4}{3}C_{t1} + \frac{2}{3}C_{t2} - 2C_{t3} - \frac{4}{3}\right)\beta_t, \quad (53)$$

$$\frac{d\gamma_t}{dl} = \frac{1}{3}(C_{t2} - C_{t1} + 1)\gamma_t. \quad (54)$$

IV. RESIDUE Z_f AND FERMION DAMPING RATE

In this section, we present the numerical solutions of the RG equations derived in the last section, and examine whether double- and triple-Weyl semimetals display breaking down of FL theory.

A. Double-Weyl fermions

The flows of Z_f, A, and v for double-Weyl fermions are shown in Fig. 1. According to Fig. 1(a), Z_f flows to zero, but at a very low speed. Therefore, the low-energy behavior only slightly deviates from the conventional FL theory. Indeed, we see from Fig. 1 that

$$\lim_{l\to\infty}\frac{\ln(1/Z_f)}{l} \to 0. \quad (55)$$

To understand the uniqueness of this behavior, we now consider the following residue

$$\lim_{l\to\infty}\frac{\ln(1/Z_f)}{l} \to \eta_1, \quad (56)$$

where η_1 is a finite positive constant. Based on Eq. (2) and the relation $\omega = \omega_0 e^{-l}$, where ω_0 is certain initial value, it is easy to get

$$\mathrm{Re}\Sigma^R(\omega) \sim \omega^{1-\eta_1}. \quad (57)$$

By virtue of KK relation, it is straightforward to obtain the imaginary part of retarded self-energy

$$\mathrm{Im}\Sigma^R(\omega) \sim \omega^{1-\eta_1}. \quad (58)$$

Since $\eta_1 > 0$, the corresponding fermion damping effect is stronger than a MFL, and thus signals a normal violation of conventional FL theory. We can clearly see that, the residue of double-Weyl fermions given by Eq. (55) is in sharp contrast to the standard non-FL behavior given by Eq. (56).

As shown in Fig. 1(c), the dependence of Z_f on l can be approximately written as

$$\lim_{l\to\infty}\frac{\ln(1/Z_f)}{\ln(l)} \to \eta_2, \quad (59)$$

where η_2 is a constant fulfilling the condition $0 < \eta_2 < 1$. In the long wavelength limit, the residue Z_f depends on l as follows

$$Z_f \sim \frac{1}{(l)^{\eta_2}}. \quad (60)$$

The real and imaginary parts of retarded self-energy are found to behave as

$$\mathrm{Re}\Sigma^R(\omega) \sim \omega\left[\ln\left(\frac{\omega_0}{\omega}\right)\right]^{\eta_2}, \quad (61)$$

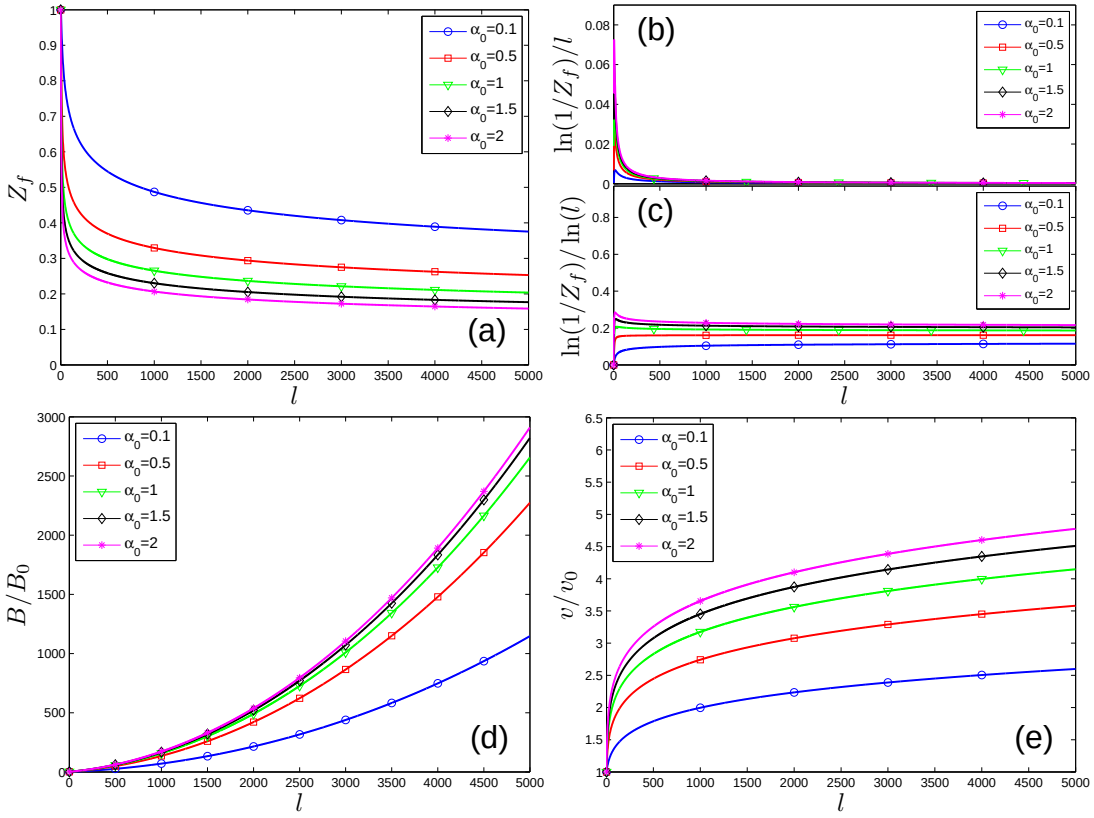

FIG. 3: Flow of Z_f, B, and v in triple-Weyl semimetal at different values of α_0. Here, $N = 2$, $\beta_{t0} = 1$, and $\gamma_{t0} = 0.2$.

and

$$\mathrm{Im}\Sigma^R(\omega) \sim \frac{|\omega|}{\left[\ln\left(\frac{\omega_0}{\omega}\right)\right]^{1-\eta_2}}. \tag{62}$$

In the special case of $\eta_2 = 1$, this corresponds to the standard MFL behavior:

$$\mathrm{Im}\Sigma^R(\omega) \sim |\omega|. \tag{63}$$

In the current case, $0 < \eta_2 < 1$, which implies that

$$\lim_{\omega\to 0} \frac{\mathrm{Im}\Sigma^R(\omega)}{\omega} \to 0. \tag{64}$$

Therefore, the Landau damping of double-Weyl fermions is actually weaker than a MFL, but the residue $Z_f \to 0$ and the conventional FL description breaks down.

As shown in Fig. 1 (c) and (d), both A and v increase with lowering energy, which is consistent with the results obtained in the RG analysis based on instantaneous approximation [40, 41]. This leads to the suppression of such observable quantities as specific heat, compressibility, and conductivity, and also to the enhancement of diamagnetic susceptibility [40, 41].

For different values of N, β_{d0}, and γ_{d0}, we depict the flows of Z_f in Fig. 2. We observe that the asymptotic behaviors of $\lim_{l\to\infty} Z_f \to 0$ and $\lim_{l\to\infty} \ln(1/Z_f)/\ln(l) \to \eta_2$ are not altered qualitatively by choosing other initial values of N, β_0, and γ_{d0}. It thus appears that Z_f is insensitive to the changes of β_{d0} and γ_{d0}. However, at given values of γ_{d0}, β_{d0}, and α_{d0}, Z_f exhibits obvious quantitative difference for $N = 2$ and $N = 4$. According to the numerical results shown in Fig. 1 and Fig. 2, the anomalous violation of FL theory is a robust phenomenon.

B. Triple-Weyl fermions

For triple-Weyl fermions, the flows of Z_f, B, and v are displayed in Fig. 3. According to Fig. 3(a) and (b), Z_f also flows to zero very slowly, which can be approximately described by Eq. (60) with $0 < \eta_2 < 1$. Similar to double-Weyl semimetal, the triple-Weyl semimetal also manifests weak violation of conventional FL description. Comparing Figs. 3(a-b) with Figs. 1(a-b), we find that the asymptotic behaviors of Z_f are nearly the same in triple- and double-Weyl semiemtals, as long as the model parameters are chosen to be the same. Fig. 3(c-d) show that both B and v increase as one goes to low energies, which is consistent with recent RG studies based on the instantaneous approximation [42]. Comparing Figs. 3(c-d) to Figs. 1(c-d), we find that, under similar conditions, the curves of B and v for triple-Weyl fermions are obviously different from A and v for double-Weyl fermions.

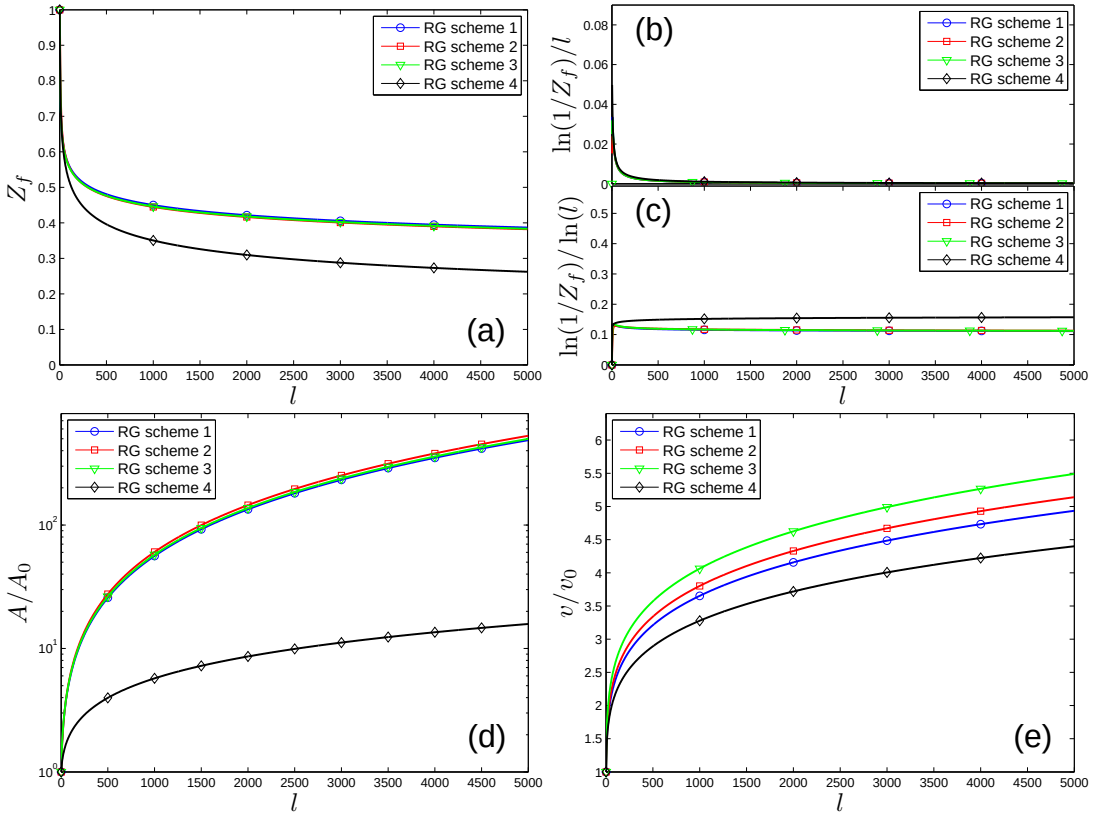

FIG. 4: Flow of Z_f, A, and v for the double-Weyl fermions under the influence of long-range Coulomb interaction in different RG schemes. $N = 2$, $\alpha_0 = 1$, $\beta_{t0} = 1$ and $\gamma_{t0} = 0.2$ are taken.

V. DIFFERENT RG SCHEMES

RG theory has been applied to study the influence of long-range Coulomb interaction on various semimetals in which the fermion dispersion depends on different components of momentum in different ways [40–42, 61, 76, 87]. However, there exists considerable ambiguity about the choice of an appropriate RG scheme. In a recent RG investigation of 3D ani-Weyl semimetal, the quadratic momentum component was used to define a shell and then integrated out [76]. Isobe *et al.* [61] carried out a RG analysis of 2D semi-Dirac semimetal by integrating over a energy shell. In contrast, when studying 2D semi-Dirac semimetal, Cho and Moon [87] employed a momentum shell for the linear momentum component. In the case of double-Weyl semimetal, Lai [40] chose to define a shell for quadratic momentum components, whereas Jian and Yao [41] introduced a range of $b\Lambda < E < \Lambda$ with $E = \sqrt{A^2k_\perp^4 + v^2k_z^2}$. A subsequent RG study of triple-Weyl semimetal [42] considered a similar RG scheme $b\Lambda < E < \Lambda$, where $E = \sqrt{B^2k_\perp^6 + v^2k_z^2}$. It is important to notice that different RG schemes may lead to different results [40, 41]. It is therefore of some interest to study the same model by means of these RG schemes, and then make a direct comparison between the results.

In the above calculations, we have used the RG schemes previously employed in Refs. [40, 41]. To examine whether our conclusion is altered by other ways of performing RG integration, we re-derive the RG equations and analyze the solutions by means of three different RG schemes. In addition to the RG scheme defined by Eq. (16) or Eq. (37), which is named as RG scheme 1 (RGS1), we also consider the following three schemes:

$$\int'_{\Omega,q} = \int_{-\infty}^{+\infty} d\Omega \int_{\Lambda_1}^{\Lambda} dq_\perp q_\perp \int_{-\infty}^{+\infty} dq_z, \tag{65}$$

$$\int'_{\Omega,q} = \int_{-\infty}^{+\infty} d\Omega \int_{0}^{+\infty} dq_\perp q_\perp \left(\int_{-\Lambda}^{-b\Lambda} + \int_{b\Lambda}^{\Lambda}\right) dq_z, \tag{66}$$

$$\int'_{\Omega,q} = \left(\int_{-\Lambda}^{-b\Lambda} + \int_{b\Lambda}^{\Lambda}\right) d\Omega \int_{0}^{+\infty} dq_\perp q_\perp \int_{-\infty}^{+\infty} dq_z, \tag{67}$$

where $\int'_{\Omega,q} \equiv \int' d\Omega dq_\perp q_\perp dq_z$. The cutoff $\Lambda_1 = \sqrt{b}\Lambda$ for double-Weyl semimetal, and $\Lambda_1 = b^{\frac{1}{3}}\Lambda$ for triple-Weyl semimetal. For simplicity, we name Eq. (65), Eq. (66), and Eq. (67) as RGS2, RGS3, and RGS4, respectively.

A. Double-Weyl semimetal

For double-Weyl semimetal, the self-energy is independent of RG scheme and is always formally expressed by

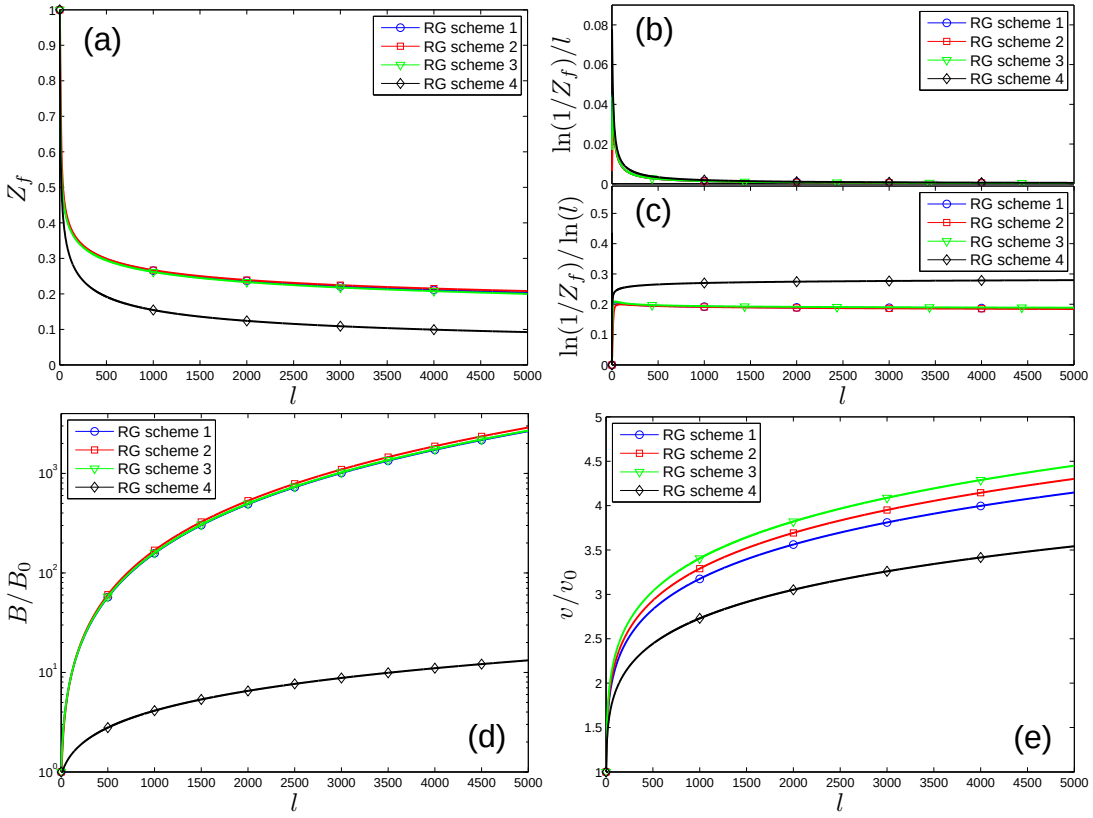

FIG. 5: Flow of Z_f, B, and v for triple-Weyl fermions obtained by using different RG schemes. Here, $N = 2$, $\alpha_0 = 1$, $\beta_{t0} = 1$, and $\gamma_{t0} = 0.2$.

Eq. (17). The RG equations for parameters Z_f, A, v, and α are still given by Eqs. (49)-(52). The expressions for $C_{d,i} \equiv C_{d,i}(\alpha, \beta_d, \gamma_d)$ obtained by using RGS2, RGS3, and RGS4 are presented in Appendix E 1.

For RGS2, the parameters β_d and γ_d are defined as

$$\beta_d = \frac{A\Lambda}{v}, \quad \gamma_d = \frac{\Lambda_{UV}}{\Lambda}. \tag{68}$$

The corresponding RG equations for β_d and γ_d are given by

$$\frac{d\beta_d}{dl} = \left(C_{d2} - C_{d3} - \frac{1}{2}\right)\beta_d, \tag{69}$$

$$\frac{d\gamma_d}{dl} = \frac{1}{2}\gamma_d. \tag{70}$$

For RGS3, β_d and γ_d can be written as

$$\beta_d = \frac{A\Lambda}{v}, \quad \gamma_d = \frac{\sqrt{A}\Lambda_{UV}}{\sqrt{v\Lambda}}. \tag{71}$$

Accordingly, their RG equations have the form

$$\frac{d\beta_d}{dl} = (C_{d2} - C_{d3} - 1)\,\beta_d, \tag{72}$$

$$\frac{d\gamma_d}{dl} = \frac{1}{2}(C_{d2} - C_{d3} + 1)\,\gamma_d. \tag{73}$$

For RGS4, β_d and γ_d are still defined as Eq. (18), and their RG equations are also given by Eq. (34) and Eq. (35).

We present the numerical results for the flows of Z_f, A, and v in Fig. 4. According to Fig. 4(a) and Fig. 4(b), Z_f exhibits nearly the same qualitative behavior in the cases of different RG schemes. Therefore, the abnormal violation of FL description in double-Weyl semimetal is independent of the specific scheme chosen to perform RG calculations. Quantitatively, the curves for $Z_f(l)$ obtained by using RGS1, RGS2, and RGS3 are very close to each other. However, the curve of $Z_f(l)$ obtained by using RGS4 is noticeably different. As shown in Fig. 4(c) and Fig. 4(d), A and v always increase with lowering energy, but the curve of $A(l)$ in the case of RGS4 is markedly different from the other three cases.

B. Triple-Weyl semimetal

The self-energy of triple-Weyl fermions is always formally given by Eq. (38). The parameters Z_f, B, v, and α still satisfy Eqs. (49)-(52). The expressions of $C_{ti} \equiv C_{ti}(\alpha, \beta_t, \gamma_t)$ obtained by using RGS2, RGS3, and RGS4 are presented in Appendix E 2.

For RGS2, the parameters β_t and γ_t are defined as

$$\beta_t = \frac{B\Lambda^2}{v}, \quad \gamma_t = \frac{\Lambda_{UV}}{\Lambda}. \tag{74}$$

Their RG equations are

$$\frac{d\beta_t}{dl} = \left(C_{t2} - C_{t3} - \frac{2}{3}\right)\beta_t, \tag{75}$$

$$\frac{d\gamma_t}{dl} = \frac{1}{3}\gamma_t. \tag{76}$$

For RGS3, we have

$$\beta_t = \frac{B^{\frac{2}{3}}\Lambda^{\frac{4}{3}}}{v^{\frac{2}{3}}}, \quad \gamma_t = \frac{B^{\frac{1}{3}}\Lambda_{UV}}{(v\Lambda)^{\frac{1}{3}}}. \tag{77}$$

The corresponding RG equations become

$$\frac{d\beta_t}{dl} = \frac{2}{3}\left(C_{t2} - C_{t3} - 2\right)\beta_t, \tag{78}$$

$$\frac{d\gamma_t}{dl} = \frac{1}{3}\left(C_{t2} - C_{t3} + 1\right)\gamma_t. \tag{79}$$

For RGS4, β and γ_t have the same definitions as RGS1, given by Eq. (39), and the RG equations still satisfy Eq. (53) and Eq. (54).

The flows of Z_f, B, and v for triple-Weyl semimetal are shown in Fig. 5. Similar to the case of double-Weyl semimetal, we still find anomalous violation of conventional FL description are qualitatively independent of the RG scheme. However, the curve $Z_f(l)$ obtained by using RGS4 is quantitatively obviously different from other cases. The asymptotic behaviors of B and v are also qualitatively the same in the cases of four RG schemes. Similar to the parameter A in double-Weyl semimetal, there is an apparent deviation of the curve of $B(l)$ for RGS4 from other three RG schemes.

VI. SUMMARY AND DISCUSSION

In summary, we have studied the low-energy behaviors of quasiparticle residue Z_f and fermion damping rate of double- and triple-Weyl fermions by performing a detailed RG analysis. Comparing to previous related works, we have taken into account the impact of dynamical screening on the long-range Coulomb interaction. After solving the RG equations for all the model parameters, we have found a new type of state that invalidates FL theory in an anomalous way, in which the residue Z_f flows to zero very slowly in the lowest energy limit and the fermion damping is weaker than a rigorous MFL. Such state provides a weaker deviation of conventional FL theory than MFL.

In a recent work, we have investigated the strong coupling between the gapless nodal fermions and the critical quantum fluctuation of nematic order parameter inside the superconducting dome of cuprates [96]. In that case, the residue Z_f also flows to zero at a very low speed, similar to the anomalous violation of FL theory predicted in this paper. Since the cuprate samples are often not sufficiently clean, it would be practically difficult to probe such an anomalous NFL state in experiments. In contrast, it would be technically easier to prepare clean double- and triple-Weyl semimetal samples. We therefore expect future ARPES experiments [94, 95] could be performed to detect the non-standard NFL behaviors in these two types of material.

Another interesting possibility is that a finite gap might be dynamically generated at the band-touching point by a sufficiently strong Coulomb interaction. This would lead to a semimetal-insulator quantum phase transition [12, 62, 73, 81, 84, 85] and a series of intriguing quantum critical phenomena [62]. Since the Coulomb interaction plays a significant role over a wide range of energy scales, there is a good opportunity for such an insulating transition to occur. This possibility will be studied in a separate work in the future.

ACKNOWLEDGEMENTS

We would like to acknowledge the financial support by National key Research and Development Program of China under Grant No. 2016YFA0300404, and the support by the National Natural Science Foundation of China under Grants 11504379, 11274286, 11574285, 11674327, and U1532267. J.R.W. is also supported by the Natural Science Foundation of Anhui Province under Grant 1608085MA19.

Appendix A: Polarization $\Pi_d(\omega, \mathbf{q})$ of double-Weyl fermions

In the case of double-Weyl fermions, the polarization is defined as

$$\Pi_d(\Omega, \mathbf{q}) = -N \int \frac{d\omega}{2\pi} \int \frac{d^3\mathbf{k}}{(2\pi)^3} \mathrm{Tr}\left[G_{d0}(\omega, \mathbf{k}) G_{d0}\left(\omega + \Omega, \mathbf{k} + \mathbf{q}\right)\right] \tag{A1}$$

to the leading order of $1/N$ expansion. Substituting the expression of fermion propagator Eq. (6) into Eq. (A1), one gets

$$\Pi_d\left(\Omega, \frac{q_x}{\sqrt{A}}, \frac{q_y}{\sqrt{A}}, \frac{q_z}{v}\right) = \frac{2N}{Av} \int \frac{d\omega}{2\pi} \int \frac{d^3\mathbf{k}}{(2\pi)^3} \frac{\omega\left(\omega + \Omega\right) - d_1(\mathbf{k}) d_1(\mathbf{k}+\mathbf{q}) - d_2(\mathbf{k}) d_2\left(\mathbf{k}+\mathbf{q}\right) - k_z\left(k_z + q_z\right)}{\left(\omega^2 + E_{\mathbf{k}}^2\right)\left[\left(\omega + \Omega\right)^2 + E_{\mathbf{k}+\mathbf{q}}^2\right]}, \tag{A2}$$

where $d_1(\mathbf{k}) = k_x^2 - k_y^2$, $d_2(\mathbf{k}) = 2k_x k_y$ and $E_k = \sqrt{k_\perp^4 + k_z^2}$. This expression is obtained by making the following re-scaling manipulations:

$$k_x \to \frac{k_x}{\sqrt{A}}, \quad q_x \to \frac{q_x}{\sqrt{A}}, \quad k_y \to \frac{k_y}{\sqrt{A}}, \quad q_y \to \frac{q_y}{\sqrt{A}}, \quad k_z \to \frac{k_z}{v}, \quad q_z \to \frac{q_z}{v}. \tag{A3}$$

Employing the Feynman parameterization

$$\frac{1}{XY} = \int_0^1 dx \frac{1}{\left[xX + (1-x)Y\right]^2}, \tag{A4}$$

the polarization can be further written as

$$\begin{aligned}\Pi_d(\Omega, \frac{q_x}{\sqrt{A}}, \frac{q_y}{\sqrt{A}}, \frac{q_z}{v}) &= \frac{2N}{Av} \int_0^1 dx \int \frac{dk_x}{2\pi} \frac{dk_y}{2\pi} \Big[-x(1-x)\left(\Omega^2 - q_z^2\right) - d_1\left(\mathbf{k} - \frac{\mathbf{q}}{2}\right) d_1\left(\mathbf{k} + \frac{\mathbf{q}}{2}\right) - d_2\left(\mathbf{k} - \frac{\mathbf{q}}{2}\right) \\ &\times\ d_2\left(\mathbf{k} + \frac{\mathbf{q}}{2}\right)\Big] \int \frac{d^2\mathbf{K}}{(2\pi)^2} \frac{1}{\left[K^2 + x(1-x)\left(\Omega^2 + q_z^2\right) + (1-x)\left(\mathbf{k} - \frac{\mathbf{q}}{2}\right)^4 + x\left(\mathbf{k} + \frac{\mathbf{q}}{2}\right)_\perp^4\right]^2},\end{aligned} \tag{A5}$$

where $K = (\omega, k_z)$, and the transformations $k_x \to k_x - \frac{q_x}{2}$ and $k_y \to k_y - \frac{q_y}{2}$ have been made. Performing the integration over K by using the formula

$$\int \frac{d^dQ}{(2\pi)^d} \frac{1}{\left(Q^2 + \Delta\right)^n} = \frac{1}{(4\pi)^{d/2}} \frac{\Gamma\left(n - d/2\right)}{\Gamma(n)} \frac{1}{\Delta^{n-d/2}}, \tag{A6}$$

we get

$$\begin{aligned}\Pi_d(\Omega, \frac{q_x}{\sqrt{A}}, \frac{q_y}{\sqrt{A}}, q_z) &= \frac{N}{2\pi Av} \int_0^1 dx \int \frac{dk_x}{2\pi} \frac{dk_y}{2\pi} \Bigg\{\Bigg[-x(1-x)\left(\Omega^2 - q_z^2\right) - \left(k_\perp^2 - \frac{q_\perp^2}{4}\right)^2 + \left(k_y q_x - k_x q_y\right)^2\Bigg] \\ &\times \Bigg[x(1-x)\left(\Omega^2 + q_z^2\right) + \left(k_\perp^2 + \frac{q_\perp^2}{4}\right)^2 + \left(k_x q_x + k_y q_y\right)^2 \\ &-2(1-2x)\left(k_\perp^2 + \frac{q_\perp^2}{4}\right)\left(k_x q_x + k_y q_y\right)\Bigg]^{-1} + 1\Bigg\}.\end{aligned} \tag{A7}$$

This polarization has already been regularized by replacing $\Pi_d(\Omega, \frac{q_x}{\sqrt{A}}, \frac{q_y}{\sqrt{A}}, \frac{q_z}{v})$ with $\Pi_d(\Omega, \frac{q_x}{\sqrt{A}}, \frac{q_y}{\sqrt{A}}, \frac{q_z}{v}) - \Pi_d(0,0,0,0)$. We now introduce the polar coordinates, and re-write the polarization as

$$\begin{aligned}\Pi_d(\Omega, \frac{q_\perp}{\sqrt{A}}, q_z) &= \frac{N}{8\pi^3 Av} \int_0^1 dx \int_0^{\Lambda_{UV}} dk_\perp k_\perp \int_0^{2\pi} d\theta \\ &\times \left[\frac{-x(1-x)\left(\Omega^2 - q_z^2\right) - \left(k_\perp^2 - \frac{q_\perp^2}{4}\right)^2 + k_\perp^2 q_\perp^2 \sin^2\theta}{x(1-x)\left(\Omega^2 + q_z^2\right) + \left(k_\perp^2 + \frac{q_\perp^2}{4}\right)^2 + k_\perp^2 q_\perp^2 \cos^2\theta - 2(1-2x)\left(k_\perp^2 + \frac{q_\perp^2}{4}\right) k_\perp q_\perp \cos\theta} + 1\right]\end{aligned} \tag{A8}$$

where is θ is the angle between $\mathbf{k}_\perp$ and $\mathbf{q}_\perp$, and Λ_{UV} is a cutoff. This polarization function is formally very complicated, and cannot be directly used to calculate the fermion self-energy function. It is helpful to analyze its asymptotic behaviors in several different limits, and then obtain an approximate expression of the polarization.

1. $q_\perp = 0$

In the limit $q_\perp = 0$, the polarization takes the form

$$\begin{aligned}\Pi_d(\Omega, 0, \frac{q_z}{v}) &= \frac{N}{8\pi^3 Av}\int_0^1 dx \int_0^{\Lambda_{UV}} dk_\perp k_\perp \int_0^{2\pi} d\theta \left[\frac{-x(1-x)\left(\Omega^2 - q_z^2\right) - k_\perp^4}{x(1-x)\left(\Omega^2 + q_z^2\right) + k_\perp^4} + 1\right] \\ &= \frac{N}{2\pi^2 Av} q_z^2 \int_0^1 dx x(1-x) \int_0^{\Lambda_{UV}} dk_\perp k_\perp \frac{1}{x(1-x)\left(\Omega^2 + q_z^2\right) + k_\perp^4}. \end{aligned} \tag{A9}$$

The upper limit of the integration over $k_\perp$ can be taken to be infinity, which means that

$$\Pi_d(\Omega, 0, \frac{q_z}{v}) = \frac{N}{4\pi^2 Av} q_z^2 \int_0^1 dx x(1-x) \int_0^{+\infty} dk_\perp k_\perp \frac{1}{x(1-x)\left(\Omega^2 + q_z^2\right) + k_\perp^4} = \frac{N}{64Av} \frac{q_z^2}{\sqrt{\Omega^2 + q_z^2}}. \tag{A10}$$

2. $\Omega = 0$ and $q_z = 0$

Setting $\Omega = 0$ and $q_z = 0$, we simplify the polarization to

$$\begin{aligned}\Pi_d(0, \frac{q_\perp}{\sqrt{A}}, 0) &= \frac{N}{8\pi^3 Av}\int_0^1 dx \int_0^{\Lambda_{UV}} dk_\perp k_\perp \int_0^{2\pi} d\theta \\ &\times \left[\frac{-\left(k_\perp^2 - \frac{q_\perp^2}{4}\right)^2 + k_\perp^2 q_\perp^2 \sin^2(\theta)}{\left(k_\perp^2 + \frac{q_\perp^2}{4}\right)^2 + k_\perp^2 q_\perp^2 \cos^2\theta - 2(1-2x)\left(k_\perp^2 + \frac{q_\perp^2}{4}\right) k_\perp q_\perp \cos(\theta)} + 1\right]. \end{aligned} \tag{A11}$$

Carrying out the integration over x, and using the transformation $k_\perp = q_\perp y$, we obtain

$$\Pi_d(0, \frac{q_\perp}{\sqrt{A}}, 0) = \frac{N}{8\pi^3 Av} q_\perp^2 \int_0^{\frac{\pi}{2}} d\theta \int_0^{\frac{\Lambda_{UV}}{q_\perp}} dy \left[2\frac{-\left(y^2 - \frac{1}{4}\right)^2 + y^2 \sin^2(\theta)}{\left(y^2 + \frac{1}{4}\right)\cos(\theta)} \ln\left(\frac{y^2 + \frac{1}{4} + y\cos(\theta)}{y^2 + \frac{1}{4} - y\cos(\theta)}\right) + 4y\right]. \tag{A12}$$

In the limit $y \to \infty$, it is easy to verify that

$$2\frac{-\left(y^2 - \frac{1}{4}\right)^2 + y^2 \sin^2(\theta)}{\left(y^2 + \frac{1}{4}\right)\cos(\theta)} \ln\left(\frac{y^2 + \frac{1}{4} + y\cos(\theta)}{y^2 + \frac{1}{4} - y\cos(\theta)}\right) + 4y \to \frac{16 - 8\cos(2\theta)}{3y}. \tag{A13}$$

In the low-energy regime, $\Pi(0, \frac{q_\perp}{\sqrt{A}}, 0)$ is given by

$$\Pi_d(0, \frac{q_\perp}{\sqrt{A}}, 0) = \frac{N}{8\pi^3 Av} q_\perp^2 \left[a_1 + a_2 + \frac{8\pi}{3}\ln\left(\frac{\Lambda_{UV}}{q_\perp}\right)\right], \tag{A14}$$

where

$$a_1 = \int_0^{\frac{\pi}{2}} d\theta \int_0^1 dy \left[2\frac{-\left(y^2 - \frac{1}{4}\right)^2 + y^2 \sin^2(\theta)}{\left(y^2 + \frac{1}{4}\right)\cos(\theta)} \ln\left(\frac{y^2 + \frac{1}{4} + y\cos(\theta)}{y^2 + \frac{1}{4} - y\cos(\theta)}\right) + 4y\right], \tag{A15}$$

$$a_2 = \int_0^{\frac{\pi}{2}} d\theta \int_1^{+\infty} dy \left[2\frac{-\left(y^2 - \frac{1}{4}\right)^2 + y^2 \sin^2(\theta)}{\left(y^2 + \frac{1}{4}\right)\cos(\theta)} \ln\left(\frac{y^2 + \frac{1}{4} + y\cos(\theta)}{y^2 + \frac{1}{4} - y\cos(\theta)}\right) + 4y - \frac{16 - 8\cos(2\theta)}{3y}\right]. \tag{A16}$$

Through numerical calculation, we find that

$$a_1 \approx 3.83504, \qquad a_2 \approx -1.4367. \tag{A17}$$

Retaining the leading contribution, the polarization is approximately written as

$$\Pi_d(0, \frac{q_\perp}{\sqrt{A}}, , 0) = \frac{N}{3\pi^2 Av} q_\perp^2 \ln\left(\frac{\Lambda_{UV}}{q_\perp}\right). \tag{A18}$$

3. $q_z = 0$ and $q_\perp^2 \ll \Omega$

In the limit $q_z = 0$, we have

$$\Pi_d(\Omega, \frac{q_\perp}{\sqrt{A}}, 0) = \frac{N}{8\pi^3 Av}\int_0^1 dx \int_0^{\Lambda_{UV}} dk_\perp k_\perp \int_0^{2\pi} d\theta \times \left[\frac{-x(1-x)\Omega^2 - \left(k_\perp^2 - \frac{q_\perp^2}{4}\right)^2 + k_\perp^2 q_\perp^2 \sin^2(\theta)}{x(1-x)\Omega^2 + \left(k_\perp^2 + \frac{q_\perp^2}{4}\right)^2 + k_\perp^2 q_\perp^2 \cos^2\theta - 2(1-2x)\left(k_\perp^2 + \frac{q_\perp^2}{4}\right) k_\perp q_\perp \cos(\theta)} + 1\right], \quad \text{(A19)}$$

If $q_\perp^2 \ll \Omega$ is satisfied, the polarization can be approximated by

$$\Pi_d(\Omega, \frac{q_\perp}{\sqrt{A}}, 0) = \frac{Nq_\perp^2}{2\pi^2 Av}\int_0^{\Lambda_{UV}} dk_\perp k_\perp^3 \left[\left(1 + 2\frac{k_\perp^4}{\Omega^2}\right)\int_0^1 dx \frac{1}{x(1-x)\Omega^2 + k_\perp^4} - \frac{2}{\Omega^2}\right]. \quad \text{(A20)}$$

Carrying out the integration of x and using the transformation $k_\perp = \sqrt{|\Omega|}y$, we get

$$\Pi_d(\Omega, \frac{q_\perp}{\sqrt{A}}, 0) = \frac{Nq_\perp^2}{\pi^2 Av}\int_0^{\frac{\Lambda_{UV}}{\sqrt{|\Omega|}}} dy y^3 \left[\frac{1+2y^4}{\sqrt{1+4y^4}} \ln\left(\frac{\sqrt{1+4y^4}+1}{\sqrt{1+4y^4}-1}\right) - 1\right]. \quad \text{(A21)}$$

As $y \to \infty$, the integrand becomes

$$y^3 \left[\frac{1+2y^4}{\sqrt{1+4y^4}} \ln\left(\frac{\sqrt{1+4y^4}+1}{\sqrt{1+4y^4}-1}\right) - 1\right] \to \frac{1}{3y}, \quad \text{(A22)}$$

which enable us to express $\Pi_d(\Omega, \frac{q_\perp}{\sqrt{A}}, 0)$ in the form

$$\Pi_d(\Omega, \frac{q_\perp}{\sqrt{A}}, 0) = \frac{Nq_\perp^2}{\pi^2 Av}\left[a_3 + a_4 + \frac{1}{3}\ln\left(\frac{\Lambda_{UV}}{\sqrt{|\Omega|}}\right)\right], \quad \text{(A23)}$$

where

$$a_3 = \int_0^1 dy y^3 \left[\frac{1+2y^4}{\sqrt{1+4y^4}} \ln\left(\frac{\sqrt{1+4y^4}+1}{\sqrt{1+4y^4}-1}\right) - 1\right], \quad \text{(A24)}$$

$$a_4 = \int_1^{+\infty} dy \left[y^3 \left[\frac{1+2y^4}{\sqrt{1+4y^4}} \ln\left(\frac{\sqrt{1+4y^4}+1}{\sqrt{1+4y^4}-1}\right) - 1\right] - \frac{1}{3y}\right]. \quad \text{(A25)}$$

Numerical calculations show that

$$a_3 \approx 0.192007, \quad a_4 \approx -0.0114519. \quad \text{(A26)}$$

Retaining the leading term, the polarization is given by

$$\Pi_d(\Omega, \frac{q_\perp}{\sqrt{A}}, 0) \approx \frac{Nq_\perp^2}{3\pi^2 Av}\ln\left(\frac{\Lambda_{UV}}{\sqrt{|\Omega|}}\right). \quad \text{(A27)}$$

4. *Ansatz* for $\Pi_d(\omega, \mathbf{q})$

According to the polarization calculated in different limits, as shown in Eqs. (A10), (A18), and (A27), we find that the polarization can be approximated by the following *Anstaz*:

$$\Pi_d(\Omega, \frac{q_\perp}{\sqrt{A}}, \frac{q_z}{v}) \approx \frac{Nq_\perp^2}{3\pi^2 Av}\ln\left(\frac{\Lambda_{UV}}{(\Omega^2 + q_\perp^4)^{\frac{1}{4}}}\right) + \frac{N}{64Av}\frac{q_z^2}{\sqrt{\Omega^2 + q_z^2}}. \quad \text{(A28)}$$

Making the re-scaling transformations

$$\frac{q_x}{\sqrt{A}} \to q_x, \quad \frac{q_y}{\sqrt{A}} \to q_y, \quad \frac{\Lambda}{\sqrt{A}} \to \Lambda, \quad \frac{q_z}{v} \to q_z, \tag{A29}$$

we get

$$\Pi_d(\Omega, q_\perp, q_z) \approx N \left[\frac{q_\perp^2}{3\pi^2 v} \ln \left(\frac{\sqrt{A}\Lambda_{UV}}{(\Omega^2 + A^2 q_\perp^4)^{\frac{1}{4}}} \right) + \frac{1}{64A} \frac{v q_z^2}{\sqrt{\Omega^2 + v^2 q_z^2}} \right]. \tag{A30}$$

If this expression is utilized to compute the fermion self-energy, there will appear an integration region that satisfies $\sqrt{\Omega^2 + A^2 q_\perp^4} \gg A\Lambda_{UV}^2$. In this region, the logarithmic function

$$\ln \left(\frac{\sqrt{A}\Lambda_{UV}}{(\Omega^2 + A^2 q_\perp^4)^{\frac{1}{4}}} \right) < 0, \tag{A31}$$

which is ill defined and induces unphysical singular poles in the dressed Coulomb interaction. In order to avoid such unphysical results, we employ the replacement

$$\ln \left(\frac{\sqrt{A}\Lambda_{UV}}{(\Omega^2 + A^2 q_\perp^4)^{\frac{1}{4}}} \right) \to \ln \left(\frac{\sqrt{A}\Lambda_{UV} + \left(\Omega^2 + A^2 q_\perp^4\right)^{\frac{1}{4}}}{(\Omega^2 + A^2 q_\perp^4)^{\frac{1}{4}}} \right). \tag{A32}$$

Finally, the polarization function can be approximately written in the form

$$\Pi_d(\Omega, q_\perp, q_z) \approx N \left[\frac{q_\perp^2}{3\pi^2 v} \ln \left(\frac{\sqrt{A}\Lambda_{UV} + \left(\Omega^2 + A^2 q_\perp^4\right)^{\frac{1}{4}}}{(\Omega^2 + A^2 q_\perp^4)^{\frac{1}{4}}} \right) + \frac{1}{64A} \frac{v q_z^2}{\sqrt{\Omega^2 + v^2 q_z^2}} \right], \tag{A33}$$

which is well defined and used to compute the fermion self-energy function in Sec. III.

Appendix B: Self-Energy of Double-Weyl fermion

To the leading order of $1/N$ expansion, the self-energy of double-Weyl fermions induced by the long-range Coulomb interaction is defined as

$$\Sigma_d(\omega, \mathbf{k}) = \int' \frac{d\Omega}{2\pi} \frac{d^3\mathbf{q}}{(2\pi)^3} G_{d0}(\omega + \Omega, \mathbf{k} + \mathbf{q}) V_d(\Omega, \mathbf{q}), \tag{B1}$$

where

$$V_d(\Omega, \mathbf{q}) = \frac{1}{V_0^{-1}(\mathbf{q}) + \Pi_d(\Omega, \mathbf{q})} = \frac{1}{\frac{|\mathbf{q}|^2}{4\pi\alpha v} + N \left[\frac{q_\perp^2}{3\pi^2 v} \ln \left(\frac{\sqrt{A}\Lambda_{UV} + \left(\Omega^2 + A^2 q_\perp^4\right)^{\frac{1}{4}}}{\left(\Omega^2 + A^2 q_\perp^4\right)^{\frac{1}{4}}} \right) + \frac{1}{64A} \frac{v q_z^2}{\sqrt{\Omega^2 + v^2 q_z^2}} \right]}. \tag{B2}$$

Substituting Eq. (6) into Eq. (B1), and then expanding $\Sigma_d(\omega, \mathbf{k})$ in powers of small values of $i\omega$, k_x, k_y, and k_z to the leading order, the above self-energy can be expressed as

$$\Sigma_d(\omega, \mathbf{k}) = (i\omega)\Sigma_{d1} - \left[A\left(k_x^2 - k_y^2\right)\sigma_x + 2Ak_x k_y \right] \Sigma_{d2} - v k_z \sigma_z \Sigma_{d3}, \tag{B3}$$

where

$$\Sigma_{d1} = \frac{1}{8\pi^3} \int' d\Omega dq_\perp q_\perp dq_z \frac{\Omega^2 - A^2 q_\perp^4 - v^2 q_z^2}{\left(\Omega^2 + A^2 q_\perp^4 + v^2 q_z^2\right)^2} V_d(\Omega, \mathbf{q}), \tag{B4}$$

$$\Sigma_{d2} = \frac{1}{8\pi^3} \int' d\Omega dq_\perp q_\perp dq_z \left[\frac{\Omega^2 - 4A^2 q_\perp^4 + v^2 q_z^2}{\left(\Omega^2 + A^2 q_\perp^4 + v^2 q_z^2\right)^2} + \frac{4A^4 q_\perp^8}{\left(\Omega^2 + A^2 q_\perp^4 + v^2 q_z^2\right)^3} \right] V_d(\Omega, \mathbf{q}), \tag{B5}$$

$$\Sigma_{d3} = \frac{1}{8\pi^3} \int' d\Omega dq_\perp q_\perp dq_z \frac{\Omega^2 + A^2 q_\perp^4 - v^2 q_z^2}{\left(\Omega^2 + A^2 q_\perp^4 + v^2 q_z^2\right)^2} V_d(\Omega, \mathbf{q}). \tag{B6}$$

There are several different schemes to perform RG re-scaling transformations. Here, we first adopt the following integration regions:

$$-\infty<\Omega<\infty, \qquad b\Lambda<E_d<\Lambda, \quad \text{with} \quad E_d=\sqrt{A^2q_\perp^4+v^2q_z^2} \tag{B7}$$

where $b=e^{-l}$. Other choices of RG scheme will be discussed in Appendix E. If we define

$$E=\sqrt{A^2q_\perp^4+v^2q_z^2}, \quad \delta=\frac{Aq_\perp^2}{v\left|q_z\right|}, \tag{B8}$$

then we can write $q_\perp$ and q_z as

$$q_\perp=\frac{\sqrt{\delta}\sqrt{E}}{\sqrt{A}\left(1+\delta^2\right)^{\frac{1}{4}}}, \quad \left|q_z\right|=\frac{E}{v\sqrt{1+\delta^2}}. \tag{B9}$$

Therefore, the integration over $q_\perp$ and q_z can be converted to the integration over E and δ, by invoking the relation

$$dq_\perp d|q_z| \;=\; \left\|\begin{array}{cc}\frac{\partial q_\perp}{\partial E} & \frac{\partial q_\perp}{\partial \delta}\\ \frac{\partial |q_z|}{\partial E} & \frac{\partial |q_z|}{\partial \delta}\end{array}\right\| dEd\delta=\left|\frac{\partial q_\perp}{\partial E}\frac{\partial |q_z|}{\partial \delta}-\frac{\partial q_\perp}{\partial \delta}\frac{\partial |q_z|}{\partial E}\right| dEd\delta=\frac{\sqrt{E}}{2v\sqrt{A}\sqrt{\delta}\left(1+\delta^2\right)^{\frac{3}{4}}}dEd\delta. \tag{B10}$$

Using the transformations given by Eqs. (B9) and (B10), we calculate Eqs. (B4)-(B4) along with the RG scheme (B7), and eventually obtain

$$\Sigma_{d1}=C_{d1}\ln(b^{-1}), \qquad \Sigma_{d2}=C_{d2}\ln(b^{-1}), \qquad \Sigma_{d3}=C_{d3}\ln(b^{-1}), \tag{B11}$$

where

$$C_{d1} \;=\; \frac{1}{8\pi^3}\int_{-\infty}^{+\infty}dx\int_0^{+\infty}d\delta\frac{1}{\left(1+\delta^2\right)^{\frac{1}{2}}}\frac{x^2-1}{\left(x^2+1\right)^2}\mathcal{G}(x,\delta), \tag{B12}$$

$$C_{d2} \;=\; \frac{1}{8\pi^3}\int_{-\infty}^{+\infty}dx\int_0^{+\infty}d\delta\frac{1}{\left(1+\delta^2\right)^{\frac{3}{2}}}\left[\frac{x^2\left(1+\delta^2\right)-4\delta^2+1}{\left(x^2+1\right)^2}+\frac{4\delta^4}{\left(1+\delta^2\right)\left(x^2+1\right)^3}\right]\mathcal{G}(x,\delta), \tag{B13}$$

$$C_{d3} \;=\; \frac{1}{8\pi^3}\int_{-\infty}^{+\infty}dx\int_0^{+\infty}d\delta\frac{1}{\left(1+\delta^2\right)^{\frac{3}{2}}}\frac{x^2\left(1+\delta^2\right)+\delta^2-1}{\left(x^2+1\right)^2}\mathcal{G}(x,\delta), \tag{B14}$$

with

$$\mathcal{G}^{-1}(x,\delta) \;=\; \frac{1}{4\pi\alpha}\left(\delta+\frac{\beta_d}{\left(1+\delta^2\right)^{\frac{1}{2}}}\right)+N\left[\frac{\delta}{3\pi^2}\ln\left(\frac{\gamma_d\left(1+\delta^2\right)^{\frac{1}{4}}}{\left(x^2\left(1+\delta^2\right)+\delta^2\right)^{\frac{1}{4}}}+1\right)+\frac{1}{64}\frac{1}{\sqrt{x^2\left(1+\delta^2\right)+1}}\right]. \tag{B15}$$

Here, β_d and γ_d are defined by $\beta_d=\frac{A\Lambda}{v^2}$ and $\gamma_d=\frac{\sqrt{A}\Lambda_{UV}}{\sqrt{\Lambda}}$, respectively.

Appendix C: Polarization $\Pi_t(\omega,\mathbf{q})$ of triple-Weyl fermions

In triple-Weyl semimetals, the polarization is given by

$$\Pi_t(\Omega,\mathbf{q})=-N\int\frac{d\omega}{2\pi}\int\frac{d^3\mathbf{k}}{(2\pi)^3}\mathrm{Tr}\left[G_{t0}(\omega,\mathbf{k})G_{t0}\left(\omega+\Omega,\mathbf{k}+\mathbf{q}\right)\right]. \tag{C1}$$

Substituting the expression of fermion propagator Eq. (7) into Eq. (C1), we get

$$\Pi_t(\Omega,\frac{q_x}{B^{\frac{1}{3}}},\frac{q_y}{B^{\frac{1}{3}}},\frac{q_z}{v}) \;=\; \frac{2N}{B^{\frac{2}{3}}v}\int\frac{d\omega}{2\pi}\int\frac{d^3\mathbf{k}}{(2\pi)^3}\frac{\omega(\omega+\Omega)-g_1(\mathbf{k})g_1(\mathbf{k}+\mathbf{q})-g_2(\mathbf{k})g_2(\mathbf{k}+\mathbf{q})-k_z\left(k_z+q_z\right)}{\left(\omega^2+E_{\mathbf{k}}^2\right)\left[(\omega+\Omega)^2+E_{\mathbf{k}+\mathbf{q}}^2\right]}, \tag{C2}$$

where $g_1(\mathbf{k})=\left(k_x^3-3k_xk_y^2\right)$, $g_2(\mathbf{k})=\left(k_y^3-3k_yk_x^2\right)$, and $E_k=\sqrt{k_\perp^6+k_z^2}$. The following re-scaling manipulations

$$k_x\to\frac{k_x}{B^{\frac{1}{3}}}, \quad k_y\to\frac{k_y}{B^{\frac{1}{3}}}, \quad q_x\to\frac{q_x}{B^{\frac{1}{3}}}, \quad q_y\to\frac{q_y}{B^{\frac{1}{3}}}, \quad k_z\to\frac{k_z}{v}, \qquad q_z\to\frac{q_z}{v}, \tag{C3}$$

have been used. Through the Feynman parameterization Eq. (A4), the polarization can be further written as

$$\begin{aligned}\Pi_t(\Omega,\frac{q_x}{B^{\frac{1}{3}}},\frac{q_y}{B^{\frac{1}{3}}},\frac{q_z}{v}) &= \frac{2N}{B^{\frac{2}{3}}v}\int_0^1 dx\int\frac{dk_x}{2\pi}\frac{dk_y}{2\pi}\Big[-x(1-x)\left(\Omega^2-q_z^2\right)-g_1\left(\mathbf{k}-\frac{\mathbf{q}}{2}\right)g_1\left(\mathbf{k}+\frac{\mathbf{q}}{2}\right)\\ &\quad -g_2\left(\mathbf{k}-\frac{\mathbf{k}}{2}\right)g_2\left(\mathbf{k}+\frac{\mathbf{q}}{2}\right)\Big]\\ &\quad\times\int\frac{d^2\mathbf{K}}{(2\pi)^2}\frac{1}{\left[K^2+x(1-x)\left(\Omega^2+q_z^2\right)+(1-x)\left(\mathbf{k}-\frac{\mathbf{q}}{2}\right)_\perp^6+x\left(\mathbf{k}+\frac{\mathbf{q}}{2}\right)_\perp^6\right]^2},\end{aligned}\tag{C4}$$

where $K=(\omega,k_z)$, and the transformations $k_x\to k_x-\frac{q_x}{2}$ and $k_y\to k_y-\frac{q_y}{2}$ have been carried out. Performing the integration over K by using the formula Eq. (A6), we obtain

$$\begin{aligned}\Pi_t(\Omega,\frac{q_x}{B^{\frac{1}{3}}},\frac{q_y}{B^{\frac{1}{3}}},\frac{q_z}{v}) &= \frac{N}{2\pi B^{\frac{2}{3}}v}\int_0^1 dx\int\frac{dk_x}{2\pi}\frac{dk_y}{2\pi}\Bigg\{\Bigg[-x(1-x)\left(\Omega^2-q_z^2\right)-\left(k_\perp^2-\frac{q_\perp^2}{4}\right)^3+3\left(k_\perp^2-\frac{q_\perp^2}{4}\right)\\ &\quad\times\left(k_xq_y-k_yq_x\right)^2\Bigg]\Bigg[x(1-x)\left(\Omega^2+q_z^2\right)+\left(k_\perp^2+\frac{q_\perp^2}{4}\right)^3+3\left(k_\perp^2+\frac{q_\perp^2}{4}\right)\left(k_xq_x+k_yq_y\right)^2\\ &\quad-(1-2x)\left(3\left(k_\perp^2+\frac{q_\perp^2}{4}\right)^2\left(k_xq_x+k_yq_y\right)+\left(k_xq_x+k_yq_y\right)^3\right)\Bigg]^{-1}+1\Bigg\}.\end{aligned}\tag{C5}$$

In order to regularize the polarization, we have used $\Pi_t(\Omega,\frac{q_x}{B^{\frac{1}{3}}},\frac{q_y}{B^{\frac{1}{3}}},\frac{q_z}{v})-\Pi_t(0,0,0,0)$ to replace $\Pi_t(\Omega,\frac{q_x}{B^{\frac{1}{3}}},\frac{q_y}{B^{\frac{1}{3}}},\frac{q_z}{v})$. In the polar coordinates, the polarization can be further converted to

$$\begin{aligned}\Pi_t(\Omega,\frac{q_\perp}{B^{\frac{1}{3}}},\frac{q_z}{v}) &= \frac{N}{8\pi^3B^{\frac{2}{3}}v}\int_0^1 dx\int_0^{\Lambda_{UV}}dk_\perp k_\perp\int_0^{2\pi}d\theta\Bigg\{\Bigg[-x(1-x)\left(\Omega^2-q_z^2\right)-\left(k_\perp^2-\frac{q_\perp^2}{4}\right)^3+3\left(k_\perp^2-\frac{q_\perp^2}{4}\right)\\ &\quad\times k_\perp^2q_\perp^2\sin^2(\theta)\Bigg]\Bigg[x(1-x)\left(\Omega^2+q_z^2\right)+\left(k_\perp^2+\frac{q_\perp^2}{4}\right)^3+3\left(k_\perp^2+\frac{q_\perp^2}{4}\right)k_\perp^2q_\perp^2\cos^2(\theta)\\ &\quad-(1-2x)\left(3\left(k_\perp^2+\frac{q_\perp^2}{4}\right)^2k_\perp q_\perp\cos(\theta)+k_\perp^3q_\perp^3\cos^3(\theta)\right)\Bigg]^{-1}+1\Bigg\},\end{aligned}\tag{C6}$$

where is θ is the angle between $\mathbf{k}_\perp$ and $\mathbf{q}_\perp$, and Λ_{UV} is a cutoff. This polarization is also very complicated and will be calculated in several different limits.

1. $q_\perp=0$

In the limit $q_\perp=0$, the polarization takes the form

$$\begin{aligned}\Pi_t(\Omega,0,\frac{q_z}{v}) &= \frac{N}{8\pi^3B^{\frac{2}{3}}v}\int_0^1 dx\int_0^{\Lambda_{UV}}dk_\perp k_\perp\int_0^{2\pi}d\theta\left[\frac{-x(1-x)\left(\Omega^2-q_z^2\right)-k_\perp^6}{x(1-x)\left(\Omega^2+q_z^2\right)+k_\perp^6}+1\right]\\ &= \frac{N}{2\pi^2B^{\frac{2}{3}}v}q_z^2\int_0^1 dxx(1-x)\int_0^{\Lambda_{UV}}dk_\perp k_\perp\frac{1}{x(1-x)\left(\Omega^2+q_z^2\right)+k_\perp^6}.\end{aligned}\tag{C7}$$

Extending the upper limit of the integration over $k_\perp$ to infinity, we find that

$$\Pi_t(\Omega,0,\frac{q_z}{v})=c_t\frac{N}{B^{\frac{2}{3}}v}\frac{q_z^2}{\left(\Omega^2+q_z^2\right)^{\frac{2}{3}}},\tag{C8}$$

where

$$c_t=\frac{2^{\frac{1}{3}}\pi^{\frac{1}{2}}}{90\Gamma\left(\frac{5}{6}\right)\Gamma(\frac{2}{3})}.\tag{C9}$$

2. $\Omega = 0$ and $q_z = 0$

When $\Omega = 0$ and $q_z = 0$, the polarization can be simplified to

$$\begin{aligned}\Pi_t(0, \frac{q_\perp}{B^{\frac{1}{3}}}, 0) &= \frac{N}{8\pi^3 B^{\frac{2}{3}} v} \int_0^1 dx \int_0^{\Lambda_{UV}} dk_\perp k_\perp \int_0^{2\pi} d\theta \left\{ \left[-\left(k_\perp^2 - \frac{q_\perp^2}{4}\right)^3 + 3\left(k_\perp^2 - \frac{q_\perp^2}{4}\right) k_\perp^2 q_\perp^2 \sin^2(\theta) \right] \right. \\ &\times \left[\left(k_\perp^2 + \frac{q_\perp^2}{4}\right)^3 + 3\left(k_\perp^2 + \frac{q_\perp^2}{4}\right) k_\perp^2 q_\perp^2 \cos^2(\theta) - (1-2x) \right. \\ &\left. \left. \times \left(3\left(k_\perp^2 + \frac{q_\perp^2}{4}\right)^2 k_\perp q_\perp \cos(\theta) + k_\perp^3 q_\perp^3 \cos^3(\theta) \right) \right]^{-1} + 1 \right\}. \end{aligned} \tag{C10}$$

After integrating over x and making the transformation $k_\perp = q_\perp y$, the polarization becomes

$$\begin{aligned}\Pi_t(0, \frac{q_\perp}{B^{\frac{1}{3}}}, 0) &= \frac{N q_\perp^2}{4\pi^3 B^{\frac{2}{3}} v} \int_0^{\frac{\pi}{2}} d\theta \int_0^{\frac{\Lambda_{UV}}{q_\perp}} dy \left[3 \frac{-\left(y^2 - \frac{1}{4}\right)^3 + 3\left(y^2 - \frac{1}{4}\right) y^2 \sin^2(\theta)}{3\left(y^2 + \frac{1}{4}\right)^2 \cos(\theta) + y^2 \cos^3(\theta)} \right. \\ &\left. \times \ln\left(\frac{y^2 + \frac{1}{4} + y\cos(\theta)}{y^2 + \frac{1}{4} - y\cos(\theta)} \right) + 2y \right]. \end{aligned} \tag{C11}$$

As $y \to \infty$, the integrand can be simplified as

$$3 \frac{-\left(y^2 - \frac{1}{4}\right)^3 + 3\left(y^2 - \frac{1}{4}\right) y^2 \sin^2(\theta)}{3\left(y^2 + \frac{1}{4}\right)^2 \cos(\theta) + y^2 \cos^3(\theta)} \ln\left(\frac{y^2 + \frac{1}{4} + y\cos(\theta)}{y^2 + \frac{1}{4} - y\cos(\theta)} \right) + 2y \to \frac{6 - 3\cos(2\theta)}{y}. \tag{C12}$$

In the low-energy regime, the polarization $\Pi_t(0, \frac{q_\perp}{B^{\frac{1}{3}}}, 0)$ has the form

$$\Pi_t(0, \frac{q_\perp}{B^{\frac{1}{3}}}, 0) = \frac{N q_\perp^2}{4\pi^3 B^{\frac{2}{3}} v} \left[a_5 + a_6 + 3\pi \ln\left(\frac{\Lambda_{UV}}{q_\perp} \right) \right], \tag{C13}$$

where

$$a_5 = \int_0^{\frac{\pi}{2}} d\theta \int_0^1 dy \left[3 \frac{-\left(y^2 - \frac{1}{4}\right)^3 + 3\left(y^2 - \frac{1}{4}\right) y^2 \sin^2(\theta)}{3\left(y^2 + \frac{1}{4}\right)^2 \cos(\theta) + y^2 \cos^3(\theta)} \ln\left(\frac{y^2 + \frac{1}{4} + y\cos(\theta)}{y^2 + \frac{1}{4} - y\cos(\theta)} \right) + 2y \right], \tag{C14}$$

$$a_6 = \int_0^{\frac{\pi}{2}} d\theta \int_1^{+\infty} dy \left[3 \frac{-\left(y^2 - \frac{1}{4}\right)^3 + 3\left(y^2 - \frac{1}{4}\right) y^2 \sin^2(\theta)}{3\left(y^2 + \frac{1}{4}\right)^2 \cos(\theta) + y^2 \cos^3(\theta)} \ln\left(\frac{y^2 + \frac{1}{4} + y\cos(\theta)}{y^2 + \frac{1}{4} - y\cos(\theta)} \right) + 2y - \frac{6 - 3\cos(2\theta)}{y} \right] \tag{C15}$$

Numerical calculations yield

$$a_5 \approx 1.9333, \quad a_6 \approx -3.28925. \tag{C16}$$

Retaining the leading term, we express the polarization as

$$\Pi_t(0, \frac{q_\perp}{B^{\frac{1}{3}}}, 0) = \frac{3N q_\perp^2}{4\pi^2 B^{\frac{2}{3}} v} \ln\left(\frac{\Lambda_{UV}}{q_\perp} \right). \tag{C17}$$

3. $q_z = 0$ and $q_\perp^2 \ll \Omega$

In the limit $q_z = 0$, we find

$$\begin{aligned}\Pi_t(\Omega, \frac{q_\perp}{B^{\frac{1}{3}}}, \frac{q_z}{v}) &= \frac{N}{8\pi^3 B^{\frac{2}{3}} v} \int_0^1 dx \int_0^{\Lambda_{UV}} dk_\perp k_\perp \int_0^{2\pi} d\theta \left\{ \left[-x(1-x)\Omega^2 - \left(k_\perp^2 - \frac{q_\perp^2}{4}\right)^3 + 3\left(k_\perp^2 - \frac{q_\perp^2}{4}\right) \right. \right. \\ &\left. \times k_\perp^2 q_\perp^2 \sin^2(\theta) \right] \left[x(1-x)\Omega^2 + \left(k_\perp^2 + \frac{q_\perp^2}{4}\right)^3 + 3\left(k_\perp^2 + \frac{q_\perp^2}{4}\right) k_\perp^2 q_\perp^2 \cos^2(\theta) \right. \\ &\left. \left. -(1-2x)\left(3\left(k_\perp^2 + \frac{q_\perp^2}{4}\right)^2 k_\perp q_\perp \cos(\theta) + k_\perp^3 q_\perp^3 \cos^3(\theta) \right) \right]^{-1} + 1 \right\}. \end{aligned} \tag{C18}$$

In case $q_\perp^3 \ll \Omega$ is satisfied, the polarization can be approximated by

$$\Pi_t(\Omega, \frac{q_\perp}{B^{\frac{1}{3}}}, 0) \;=\; \frac{9Nq_\perp^2}{8\pi^2 B^{\frac{2}{3}} v} \int dk_\perp k_\perp^5 \left[\left(1 + 2\frac{k_\perp^6}{\Omega^2}\right) \int_0^1 dx \frac{1}{x(1-x)\Omega^2 + k_\perp^6} - \frac{2}{\Omega^2} \right]. \tag{C19}$$

Performing the integration over x and employing the transformation $k_\perp = |\Omega|^{\frac{1}{3}} y$, we get

$$\Pi_t(\Omega, \frac{q_\perp}{B^{\frac{1}{3}}}, 0) \;=\; \frac{9Nq_\perp^2}{4\pi^2 B^{\frac{2}{3}} v} \int_0^{\frac{\Lambda_{UV}}{|\Omega|^{\frac{1}{3}}}} dy y^5 \left[\frac{1+2y^6}{\sqrt{1+4y^6}} \ln\left(\frac{\sqrt{1+4y^6}+1}{\sqrt{1+4y^6}-1} \right) - 1 \right].$$

As $y \to \infty$, the integrand becomes

$$y^5 \left[\frac{1+2y^6}{\sqrt{1+4y^6}} \ln\left(\frac{\sqrt{1+4y^6}+1}{\sqrt{1+4y^6}-1} \right) - 1 \right] \to \frac{1}{3y}, \tag{C20}$$

which then leads us to the following simplified expression

$$\Pi_t(\Omega, \frac{q_\perp}{B^{\frac{1}{3}}}, 0) \;=\; \frac{9Nq_\perp^2}{4\pi^2 B^{\frac{2}{3}} v} \left[a_7 + a_8 + \frac{1}{3} \ln\left(\frac{\Lambda_{UV}}{|\Omega|^{\frac{1}{3}}} \right) \right], \tag{C21}$$

where

$$a_7 \;=\; \int_0^1 dy y^5 \left[\left(1+2y^6\right) \frac{1}{\sqrt{1+4y^6}} \ln\left(\frac{\sqrt{1+4y^6}+1}{\sqrt{1+4y^6}-1} \right) - 1 \right], \tag{C22}$$

$$a_8 \;=\; \int_1^{+\infty} dy \left[y^5 \left[\left(1+2y^6\right) \frac{1}{\sqrt{1+4y^6}} \ln\left(\frac{\sqrt{1+4y^6}+1}{\sqrt{1+4y^6}-1} \right) - 1 \right] - \frac{1}{3y} \right]. \tag{C23}$$

Numerical calculation find that

$$a_7 \approx 0.128005, \quad a_8 \approx -0.0076346. \tag{C24}$$

Retaining the leading term, we have

$$\Pi_t(\Omega, \frac{q_\perp}{B^{\frac{1}{3}}}, 0) \;=\; \frac{3Nq_\perp^2}{4\pi^2 B^{\frac{2}{3}} v} \ln\left(\frac{\Lambda_{UV}}{|\Omega|^{\frac{1}{3}}} \right). \tag{C25}$$

4. *Ansatz* for $\Pi(\omega, \mathbf{q})$

Based on the polarization calculated in different limits, as shown in Eqs. (C8), (C17), and (C25), the polarization can be approximated by the *anstaz*

$$\Pi_t(\Omega, \frac{q_\perp}{B^{\frac{1}{3}}}, \frac{q_z}{v}) \;=\; \frac{3Nq_\perp^2}{4\pi^2 B^{\frac{2}{3}} v} \ln\left(\frac{\Lambda_{UV}}{(\Omega^2 + q_\perp^6)^{\frac{1}{6}}} \right) + c_t \frac{N}{B^{\frac{2}{3}} v} \frac{q_z^2}{(\Omega^2 + q_z^2)^{\frac{2}{3}}}. \tag{C26}$$

Introducing the re-scaling transformations

$$\frac{q_x}{B^{\frac{1}{3}}} = q_x, \quad \frac{q_y}{B^{\frac{1}{3}}} = q_y, \quad \frac{\Lambda_{UV}}{B^{\frac{1}{3}}} = \Lambda_{UV}, \quad \frac{q_z}{v} = q_z, \tag{C27}$$

we can get

$$\Pi_t(\Omega, q_\perp, q_z) \;\approx\; N \left[\frac{3q_\perp^2}{4\pi^2 v} \ln\left(\frac{B^{\frac{1}{3}} \Lambda_{UV}}{(\Omega^2 + B^2 q_\perp^6)^{\frac{1}{6}}} \right) + c_t \frac{1}{B^{\frac{2}{3}}} \frac{v q_z^2}{(\Omega^2 + v^2 q_z^2)^{\frac{2}{3}}} \right]. \tag{C28}$$

In order to avoid the possible unphysical results caused by this expression, we borrow the method used in the case of double-Weyl semimetal and make the replacement

$$\ln\left(\frac{B^{\frac{1}{3}} \Lambda_{UV}}{(\Omega^2 + B^2 q_\perp^6)^{\frac{1}{6}}} \right) \to \ln\left(\frac{B^{\frac{1}{3}} \Lambda_{UV} + \left(\Omega^2 + B^2 q_\perp^6\right)^{\frac{1}{6}}}{(\Omega^2 + B^2 q_\perp^6)^{\frac{1}{6}}} \right). \tag{C29}$$

Now the polarization can be approximately given by

$$\Pi_t(\Omega, q_\perp, q_z) \;\approx\; N\left[\frac{3q_\perp^2}{4\pi^2 v}\ln\left(\frac{B^{\frac{1}{3}}\Lambda_{UV}+\left(\Omega^2+B^2q_\perp^6\right)^{\frac{1}{6}}}{\left(\Omega^2+B^2q_\perp^6\right)^{\frac{1}{6}}}\right)+a_1\frac{1}{B^{\frac{2}{3}}}\frac{vq_z^2}{\left(\Omega^2+v^2q_z^2\right)^{\frac{2}{3}}}\right]. \tag{C30}$$

Appendix D: Self-Energy of triple-Weyl fermions

To the leading order of $1/N$ expansion, the self-energy of triple-Weyl fermions induced by the long-range Coulomb interaction is given by

$$\Sigma_t(\omega,\mathbf{k}) \;=\; \int'\frac{d\Omega}{2\pi}\frac{d^3\mathbf{q}}{(2\pi)^3}G_{t0}(\omega+\Omega,\mathbf{k}+\mathbf{q})V_t(\Omega,\mathbf{q}), \tag{D1}$$

where

$$V_t(\Omega,\mathbf{q}) \;=\; \frac{1}{V_0^{-1}(\mathbf{q})+\Pi_t(\Omega,\mathbf{q})}=\frac{1}{\frac{|\mathbf{q}|^2}{4\pi\alpha v}+N\left[\frac{3q_\perp^2}{4\pi^2 v}\ln\left(\frac{B^{\frac{1}{3}}\Lambda_{UV}+\left(\Omega^2+B^2q_\perp^6\right)^{\frac{1}{6}}}{\left(\Omega^2+B^2q_\perp^6\right)^{\frac{1}{6}}}\right)+c_t\frac{1}{B^{\frac{2}{3}}}\frac{vq_z^2}{\left(\Omega^2+v^2q_z^2\right)^{\frac{2}{3}}}\right]} \tag{D2}$$

After substituting Eq. (7) into Eq. (D1), and expanding $\Sigma_t(\omega,\mathbf{k})$ in powers of small values of $i\omega$, k_x, k_y, and k_z to leading order, we get

$$\Sigma_t(\omega,\mathbf{k}) \;=\; i\omega\Sigma_1-\left[B\left(k_x^3-3k_xk_y^2\right)\sigma_x+B\left(k_y^3-3k_yk_x^2\right)\sigma_y\right]\Sigma_2-vk_z\sigma_z\Sigma_3 \tag{D3}$$

where

$$\Sigma_{t1} \;=\; \frac{1}{8\pi^3}\int' d\Omega dq_\perp q_\perp dq_z\frac{\Omega^2-B^2q_\perp^6-v^2q_z^2}{\left(\Omega^2+B^2q_\perp^6+v^2q_z^2\right)^2}V(\Omega,\mathbf{q}), \tag{D4}$$

$$\Sigma_{t2} \;=\; \frac{1}{8\pi^3}\int' d\Omega dq_\perp q_\perp dq_z\left[\frac{\Omega^2-18B^2q_\perp^6+v^2q_z^2}{\left(\Omega^2+B^2q_\perp^6+v^2q_z^2\right)^2}+\frac{45B^4q_\perp^{12}}{\left(\Omega^2+B^2q_\perp^6+v^2q_z^2\right)^3}-\frac{27B^6q_\perp^{18}}{\left(\Omega^2+B^2q_\perp^6+v^2q_z^2\right)^4}\right]V(\Omega,\mathbf{q}), \tag{D5}$$

$$\Sigma_{t3} \;=\; \frac{1}{8\pi^3}\int' d\Omega dq_\perp q_\perp dq_z\frac{\Omega^2+B^2q_\perp^6-v^2q_z^2}{\left(\Omega^2+B^2q_\perp^6+v^2q_z^2\right)^2}V(\Omega,\mathbf{q}). \tag{D6}$$

To make RG analysis, we consider the following range in energy:

$$-\infty<\Omega<\infty,\qquad b\Lambda<E_t<\Lambda,\quad\text{with}\quad E_t=\sqrt{B^2q_\perp^6+v^2q_z^2}. \tag{D7}$$

Making use of the definition

$$E=\sqrt{B^2q_\perp^6+v^2q_z^2},\quad \delta=\frac{Bq_\perp^3}{v\,|q_z|}, \tag{D8}$$

we re-express $q_\perp$ and q_z as

$$q_\perp=\frac{\delta^{\frac{1}{3}}E^{\frac{1}{3}}}{B^{\frac{1}{3}}\left(1+\delta^2\right)^{\frac{1}{6}}},\quad q_z=\frac{E}{v\sqrt{1+\delta^2}}. \tag{D9}$$

Now the integration over $q_\perp$ and q_z can be transformed to the integration over E and δ through the relation

$$dq_\perp d|q_z| \;=\; \left\|\begin{array}{cc}\frac{\partial q_\perp}{\partial E} & \frac{\partial q_\perp}{\partial\delta}\\ \frac{\partial|q_z|}{\partial E} & \frac{\partial|q_z|}{\partial\delta}\end{array}\right\| dEd\delta=\left|\frac{\partial q_\perp}{\partial E}\frac{\partial|q_z|}{\partial\delta}-\frac{\partial q_\perp}{\partial\delta}\frac{\partial|q_z|}{\partial E}\right|dEd\delta=\frac{E^{\frac{1}{3}}}{3vB^{\frac{1}{3}}\delta^{\frac{2}{3}}\left(1+\delta^2\right)^{\frac{2}{3}}}dEd\delta. \tag{D10}$$

By virtue of Eqs. (D9) and (D10), we calculate Eqs. (D4)-(D6) and obtain

$$\Sigma_{t1}=C_{t1}\ln(b^{-1}),\qquad \Sigma_{t2}=C_{t2}\ln(b^{-1}),\qquad \Sigma_{t3}=C_{t3}\ln(b^{-1}), \tag{D11}$$

where

$$C_{t1} = \frac{1}{12\pi^3}\int_{-\infty}^{+\infty}dx\int_0^{+\infty}d\delta\frac{1}{\delta^{\frac{1}{3}}\left(1+\delta^2\right)^{\frac{1}{2}}}\frac{x^2-1}{\left(x^2+1\right)^2}\mathcal{G}(x,\delta), \tag{D12}$$

$$C_{t2} = \frac{1}{12\pi^3}\int_{-\infty}^{+\infty}dx\int_0^{+\infty}d\delta\frac{1}{\delta^{\frac{1}{3}}\left(1+\delta^2\right)^{\frac{3}{2}}}\left[\frac{x^2\left(1+\delta^2\right)-19\delta^2+\left(1+\delta^2\right)}{\left(x^2+1\right)^2}+\frac{45\delta^4}{\left(x^2+1\right)^3\left(1+\delta^2\right)}\right.$$
$$\left.-\frac{27\delta^6}{\left(x^2+1\right)^4\left(1+\delta^2\right)^2}\right]\mathcal{G}(x,\delta), \tag{D13}$$

$$C_{t3} = \frac{1}{12\pi^3}\int_{-\infty}^{+\infty}dx\int_0^{+\infty}d\delta\frac{1}{\delta^{\frac{1}{3}}\left(1+\delta^2\right)^{\frac{3}{2}}}\frac{x^2\left(1+\delta^2\right)+\delta^2-1}{\left(x^2+1\right)^2}\mathcal{G}(x,\delta), \tag{D14}$$

with

$$\mathcal{G}(x,\delta) = \frac{1}{\frac{1}{4\pi\alpha}\left(\delta^{\frac{2}{3}}+\frac{\beta}{\left(1+\delta^2\right)^{\frac{2}{3}}}\right)+N\left[\frac{3\delta^{\frac{2}{3}}}{4\pi^2}\ln\left(\frac{\gamma\left(1+\delta^2\right)^{\frac{1}{6}}+\left(x^2\left(1+\delta^2\right)+\delta^2\right)^{\frac{1}{6}}}{\left(x^2\left(1+\delta^2\right)+\delta^2\right)^{\frac{1}{6}}}\right)+a_1\frac{1}{\left(x^2\left(1+\delta^2\right)+1\right)^{\frac{2}{3}}}\right]}. \tag{D15}$$

Here, β_t and γ_t are defined by $\beta_t=\frac{B^{\frac{2}{3}}\Lambda^{\frac{4}{3}}}{v^2}$ and $\gamma_t=\frac{B^{\frac{1}{3}}\Lambda_{UV}}{\Lambda^{\frac{1}{3}}}$, respectively.

Appendix E: Calculation of $C_{1,2,3}$ using different RG schemes

There are several possible ways to perform RG re-scaling transformations, as discussed in Sec. V. Here, we present the expressions of the constants $C_{1,2,3}$ by employing these RG schemes separately.

1. Double-Weyl Fermions

Besides RGS1, there are three other RG schemes. The self-energy of double-Weyl fermions can be still represented by Eq. (B3), but the constants $C_{1,2,3}$ have different expressions.

For RGS2, the constants C_{di} with $(i=1,2,3)$ are given by

$$C_{d1} = \frac{1}{16\pi^3}\int_{-\infty}^{+\infty}dx\int_{-\infty}^{+\infty}dy\frac{x^2-1-y^2}{\left(x^2+1+y^2\right)^2}\mathcal{G}(x,y), \tag{E1}$$

$$C_{d2} = \frac{1}{16\pi^3}\int_{-\infty}^{+\infty}dx\int_{-\infty}^{+\infty}dy\left[\frac{x^2-4+y^2}{\left(x^2+1+y^2\right)^2}+\frac{4}{\left(x^2+1+y^2\right)^3}\right]\mathcal{G}(x,y), \tag{E2}$$

$$C_{d3} = \frac{1}{16\pi^3}\int_{-\infty}^{+\infty}dx\int_{-\infty}^{+\infty}dy\frac{x^2+1-y^2}{\left(x^2+1+y^2\right)^2}\mathcal{G}(x,y), \tag{E3}$$

where

$$\mathcal{G}^{-1}(x,y)=\frac{1+\beta_d^2y^2}{4\pi\alpha}+N\left[\frac{1}{3\pi^2}\ln\left(\frac{\gamma_d+\left(x^2+1\right)^{\frac{1}{4}}}{\left(x^2+1\right)^{\frac{1}{4}}}\right)+\frac{1}{64}\frac{y^2}{\sqrt{x^2+y^2}}\right]. \tag{E4}$$

β_d and γ_d are defined by $\beta_d=\frac{A\Lambda}{v}$ and $\gamma_d=\frac{\Lambda_{UV}}{\Lambda}$, respectively.

For RGS3, we obtain

$$C_{d1} = \frac{1}{4\pi^3}\int_{-\infty}^{+\infty}dx\int_0^{+\infty}dyy\frac{x^2-y^4-1}{\left(x^2+y^4+1\right)^2}\mathcal{G}(x,y), \tag{E5}$$

$$C_{d2} = \frac{1}{4\pi^3}\int_{-\infty}^{+\infty}dx\int_0^{+\infty}dyy\left[\frac{x^2-4y^4+1}{\left(x^2+y^4+1\right)^2}+\frac{4y^8}{\left(x^2+1+y^2\right)^3}\right]\mathcal{G}(x,y), \tag{E6}$$

$$C_{3d} = \frac{1}{4\pi^3}\int_{-\infty}^{+\infty}dx\int_0^{+\infty}dyy\frac{x^2+y^4-1}{\left(x^2+y^4+1\right)^2}\mathcal{G}(x,y), \tag{E7}$$

where

$$\mathcal{G}^{-1}(x,y)=\frac{y^2+\beta_d}{4\pi\alpha}+N\left[\frac{y^2}{3\pi^2}\ln\left(\frac{\gamma_d+\left(x^2+y^4\right)^{\frac{1}{4}}}{\left(x^2+y^4\right)^{\frac{1}{4}}}\right)+\frac{1}{64}\frac{1}{\sqrt{x^2+1}}\right]. \tag{E8}$$

β_d and γ_d takes form $\beta_d=\frac{A\Lambda}{v}$ and $\gamma_d=\frac{\sqrt{A}\Lambda_{UV}}{\sqrt{v\Lambda}}$.

For RGS4, we find

$$C_{d1} = \frac{1}{4\pi^3}\int_0^{+\infty}dx\int_{-\infty}^{+\infty}dyx\frac{1-x^4-y^2}{\left(1+x^4+y^2\right)^2}\mathcal{G}(x,y), \tag{E9}$$

$$C_{d2} = \frac{1}{4\pi^3}\int_0^{+\infty}dx\int_{-\infty}^{+\infty}dyx\left[\frac{1-4x^4+y^2}{\left(1+x^4+y^2\right)^2}+\frac{4x^8}{\left(1+4x^8+y^2\right)^3}\right]\mathcal{G}(x,y), \tag{E10}$$

$$C_{d3} = \frac{1}{4\pi^3}\int_0^{+\infty}dx\int_{-\infty}^{+\infty}dyx\frac{1+x^4-y^2}{\left(1+x^4+y^2\right)^2}\mathcal{G}(x,y), \tag{E11}$$

where

$$\mathcal{G}^{-1}(x,y) = \frac{x^2+\beta_d y^2}{4\pi\alpha}+N\left[\frac{x^2}{3\pi^2}\ln\left(\frac{\gamma_d+\left(1+x^4\right)^{\frac{1}{4}}}{\left(1+x^4\right)^{\frac{1}{4}}}\right)+\frac{1}{64}\frac{y^2}{\sqrt{1+y^2}}\right]. \tag{E12}$$

β_d and γ_d satisfies $\beta_d=\frac{A\Lambda}{v^2}$ and $\gamma_d=\frac{\sqrt{A}\Lambda_{UV}}{\sqrt{\Lambda}}$.

2. Triple-Weyl Fermions

For RGS2, the constants C_{ti} with $i=1,2,3$ can be written as

$$C_{t1} = \frac{1}{24\pi^3}\int_{-\infty}^{+\infty}dx\int_{-\infty}^{+\infty}dy\frac{x^2-1-y^2}{\left(x^2+1+y^2\right)^2}\mathcal{G}(x,y), \tag{E13}$$

$$C_{t2} = \frac{1}{24\pi^3}\int_{-\infty}^{+\infty}dx\int_{-\infty}^{+\infty}dy\left[\frac{x^2-18+y^2}{\left(x^2+1+y^2\right)^2}+\frac{45}{\left(x^2+1+y^2\right)^3}-\frac{27}{\left(x^2+1+y^2\right)^4}\right]\mathcal{G}(x,y), \tag{E14}$$

$$C_{t3} = \frac{1}{24\pi^3}\int_{-\infty}^{+\infty}dx\int_{-\infty}^{+\infty}dy\frac{x^2+1-y^2}{\left(x^2+1+y^2\right)^2}\mathcal{G}(x,y), \tag{E15}$$

where

$$\mathcal{G}(x,y)=\frac{1}{\frac{1+\beta_t^2y^2}{4\pi\alpha}+N\left[\frac{3}{4\pi^2}\ln\left(\frac{\gamma_t+(x^2+1)^{\frac{1}{6}}}{(x^2+1)^{\frac{1}{6}}}\right)+c_t\frac{y^2}{(x^2+y^2)^{\frac{2}{3}}}\right]}. \tag{E16}$$

β_t and γ_t is given by $\beta_t=\frac{B\Lambda^2}{v}$ and $\gamma_t=\frac{\Lambda_{UV}}{\Lambda}$.

For RGS3, C_{ti} are found to be

$$C_{t1} = \frac{1}{4\pi^3}\int_{-\infty}^{+\infty}dx\int_{0}^{+\infty}dyy\frac{x^2-y^6-1}{\left(x^2+y^6+1\right)^2}\mathcal{G}(x,y), \tag{E17}$$

$$C_{t2} = \frac{1}{4\pi^3}\int_{-\infty}^{+\infty}dx\int_{0}^{+\infty}dyy\left[\frac{x^2-18y^6+1}{\left(x^2+y^6+1\right)^2}+\frac{45y^{12}}{\left(x^2+y^6+1\right)^3}-\frac{27y^{18}}{\left(x^2+y^6+1\right)^4}\right]\mathcal{G}(x,y), \tag{E18}$$

$$C_{t3} = \frac{1}{4\pi^3}\int_{-\infty}^{+\infty}dx\int_{0}^{+\infty}dyy\frac{x^2+y^6-1}{\left(x^2+y^6+1\right)^2}\mathcal{G}(x,y), \tag{E19}$$

where

$$\mathcal{G}(x,y) = \frac{1}{\frac{y^2+\beta_t}{4\pi\alpha}+N\left[\frac{3y^2}{4\pi^2}\ln\left(\frac{\gamma_t+(x^2+y^6)^{\frac{1}{6}}}{(x^2+y^6)^{\frac{1}{6}}}\right)+c_t\frac{1}{(x^2+1)^{\frac{2}{3}}}\right]}. \tag{E20}$$

β_t and γ_t satisfy $\beta_t = \frac{B^{\frac{2}{3}}\Lambda^{\frac{4}{3}}}{v^{\frac{2}{3}}}$ and $\gamma_t = \frac{B^{\frac{1}{3}}\Lambda_{UV}}{(v\Lambda)^{\frac{1}{3}}}$.

For RGS4, we get

$$C_{t1} = \frac{1}{4\pi^3}\int_0^{+\infty} dx \int_{-\infty}^{+\infty} dyx \frac{1-x^6-y^2}{\left(1+x^6+y^2\right)^2}\mathcal{G}(x,y), \tag{E21}$$

$$C_{t2} = \frac{1}{4\pi^3}\int_0^{+\infty} dx \int_{-\infty}^{+\infty} dyx \left[\frac{1-18x^6+y^2}{\left(1+x^6+y^2\right)^2} + \frac{45x^{12}}{\left(1+x^6+y^2\right)^3} - \frac{27x^{18}}{\left(1+x^6+y^2\right)^4}\right]\mathcal{G}(x,y), \tag{E22}$$

$$C_{t3} = \frac{1}{4\pi^3}\int_0^{+\infty} dx \int_{-\infty}^{+\infty} dyx \frac{1+x^6-y^2}{\left(1+x^6+y^2\right)^2}\mathcal{G}(x,y), \tag{E23}$$

where

$$\mathcal{G}(x,y) = \frac{1}{\frac{x^2+\beta_t y^2}{4\pi\alpha} + N\left[\frac{3x^2}{4\pi^2}\ln\left(\frac{\gamma_t+(1+x^6)^{\frac{1}{6}}}{(1+x^6)^{\frac{1}{6}}}\right) + c_t\frac{y^2}{(1+y^2)^{\frac{2}{3}}}\right]}. \tag{E24}$$

β_t and γ_t can be written as $\beta_t = \frac{B^{\frac{2}{3}}\Lambda^{\frac{4}{3}}}{v^2}$, and $\gamma_t = \frac{B^{\frac{1}{3}}\Lambda_{UV}}{\Lambda^{\frac{1}{3}}}$.

[1] G. F. Giuliani and G. Vignale, *Quantum theory of the electron liquid* (Cambridge University Press, Cambridge, 2005).
[2] P. Coleman, *Introduction to Many-Body Physics* (Cambridge University Press, Cambridge, 2015).
[3] C. M. Varma, Z. Nussinov, W. v. Saarloos, Phys. Rep. **361**, 267 (2002).
[4] C. M. Varma, P. B. Littlewood, S. Schmitt-Rink, E. Abrahams, and A. E. Ruckenstein, Phys. Rev. Lett. **63**, 1996 (1989).
[5] M. R. Norman, Science **332**, 196 (2011).
[6] B. Keimer, S. A. Kivelson, M. R. Norman, S. Uchida, and J. Zaanen, Nature **518**, 179 (2015).
[7] O. Vafek and A. Vishwanath, Annu. Rev. Condens. Matter Phys. **5**, 83 (2014).
[8] T. O. Wehling, A. M. Black-Schaffer, and A. V. Balatsky, Adv. Phys. **63**, 1 (2014).
[9] H. Weng, X. Dai, and Z. Fang, J. Phys.:Condens. Matter **28**, 303001 (2016).
[10] A. A. Burkov, Nat. Mater. **15**, 1145 (2016).
[11] B. Yan and C. Felser, arXiv:1611.04182v1.
[12] V. N. Kotov, B. Uchoa, V. M. Pereira, F. Guinea, and A. H. Castro Neto, Rev. Mod. Phys. **84**, 1067 (2012).
[13] J. González, F. Guinea, and M. A. H. Vozmediano, Phys. Rev. Lett. **77**, 3589 (1996).
[14] J. González, F. Guinea, and M. A. H. Vozmediano, Phys. Rev. B **59**, 2474(R) (1999).
[15] J. Hofmann, E. Barnes, and S. Das Sarma, Phys. Rev. Lett. **113**, 105502 (2014).
[16] X. Wan, A. M. Turner, A. Vishwanath, and S. Y. Savrasov, Phys. Rev. B **83**, 205101 (2011).
[17] S.-M. Huang, S.-Y. Xu, I. Belopolski, C.-C. Lee, C. Chang, B. Wang, N. Alidoust, G. Bian, M. Neupane, C. Zhang, S. Jia, A. Bansil, H. Lin, M. Z. Hasan, Nat. Commun. **6**. 7373 (2015).
[18] H. Weng, C. Fang, Z. Fang, B. A. Bernevig, and X. Dai, Phys. Rev. X **5**, 011029 (2015).
[19] S.-Y. Xu, I. Belopolski, N. Alidoust, M. Neupane, G. Bian, C. Zhang, R. Sankar, G. Chang, Z. Yuan, C.-C. Lee, S.-M. Huang, H. Zheng, J. Ma, D. S. Sanchez, B. Wang, A. Bansil, F. Chou, P. P. Shibayev, H. Lin, S. Jia, and M. Z. Hasan, Science **349**, 613 (2015).
[20] B. Q. Lv, H. M. Weng, B. B. Fu, X. P. Wang, H. Miao, J. Ma, P. Richard, X. C. Huang, L. X. Zhao, G. F. Chen, Z. Fang, X. Dai, T. Qian, and H. Ding, Phys. Rev. X **5**, 031013 (2015).
[21] B. Q. Lv, N. Xu, H. M. Weng, J. Z. Ma, P. Richard, X. C. Huang, L. X. Zhao, G. F. Chen, C. E. Matt, F. Bisti, V. N. Strocov, J. Mesot, Z. Fang, X. Dai, T. Qian, M. Shi, and H. Ding, Nat. Phys. **11**, 724 (2015).
[22] L. X. Yang, Z. K. Liu, Y. Sun, H. Peng, H. F. Yang, T. Zhang, B. Zhou, Y. Zhang, Y. F. Guo, M. Rahn, D. Prabhakaran, Z. Hussain, S.-K. Mo, C. Felser, B. Yan, and Y. L. Chen, Nat. Phys. **11**, 728 (2015).
[23] S.-Y. Xu, N. Alidoust, I. Belopolski, Z. Yuan, G. Bian, T.-R. Chang, H. Zheng, V. N. Strocov, D. S. Sanchez, G. Chang, C. Zhang, D. Mou, Y. Wu, L. Huang, C.-C. Lee, S.-M. Huang, B. Wang, A. Bansil, H.-T. Jeng, T. Neupert, A. Kaminski, H. Lin, S. Jia, and M. Z. Hasan, Nat. Phys. **11**, 748 (2015).
[24] S.-Y. Xu, I. Beloposki, D. S. Sanchez, C. Zhang, G. Chang, C. Guo, G. Bian, Z. Yuan, H. Lu, T.-R. Chang, P. P. Shibayev, M. L. Prokopovych, N. Alidoust, H. Zheng, C.-C. Lee, S.-M. Huang, R. Sankar, F. Chou, C.-H. Hsu, H.-T. Jeng, A. Bansil, T. Neupert, V. N. Strocov, H. Lin, S. Jia, and M. Z. Hasan, Sci. Adv. **1**, 1501092 (2015).
[25] N. Xu, H. M. Weng, B. Q. Lv, C. E. Matt, J. Park, F. Bisti, V. N. Strocov, D. Gawryluk, E. Pomjakushina, K. Conder, N. C. Plumb, M. Radovic, G. Autès, O. V. Yazyev, Z. Fang, X. Dai, T. Qian, J. Mesot, H. Ding, and M. Shi, Nat. Commun. **7**, 11006 (2016).
[26] D.-F. Xu, Y.-P. Du, Z. Wang, Y.-P. Li, X.-H. Niu, Q.

Yao, P. Dudin, Z.-A. Xu, X.-G. Wan, and D.-L. Feng, Chin. Phys. Lett. **32**, 107101 (2015).
[27] S. Souma, Z. Wang, H. Kotaka, T. Sato, K. Nakayama, Y. Tanaka, H. Kimizuka, T. Takahashi, K. Yamauchi, T. Oguchi, K. Segawa, and Y. Ando, Phys. Rev. B **93**, 161112(R) (2016).
[28] J. Ruan, S.-K. Jian, H. Yao, H. Zhang, S.-C. Zhang, and D. Xing, Nat. Commun. **7**, 11136 (2016).
[29] J. Ruan, S.-K. Jian, D. Zhang, H. Yao, H. Zhang, S.-C. Zhang, D. Xing, Phys. Rev. Lett. **116**, 226801 (2016).
[30] G. Xu, H. Weng, Z. Wang, X. Dai, and Z. Fang, Phys. Rev. Lett. **107**, 1869806 (2011).
[31] C. Fang, M. J. Gilbert, X. Dai, and B. A. Bernevig, Phys. Rev. Lett. **108**, 266802 (2012).
[32] B.-J. Yang and N. Nagaosa, Nat. Commun. **5**, 4898 (2014).
[33] B. Bradlyn, J. Carno, Z. Wang, M. G. Vergniory, C. Felser, R. J. Cava, B. A. Bernevig, Science **353**, aaf5037 (2016).
[34] Z. Gao, M. Hua, H. Zhang, and X. Zhang, Phys. Rev. B **93**, 205109 (2016).
[35] S.-M. Huang, S.-Y. Xu, I. Belopolski, C.-C. Lee, G. Chang, T.-R. Chang, B. Wang, N. Alidoust, G. Bian, M. Neupane, D. Sanchez, H. Zheng, H.-T. Jeng, A. Bansil, T. Neupert, H. Lin, and M. Z. Hasan, Proc. Natl. Acad. Sci. U.S.A. **113**, 1180 (2016).
[36] T. Guan, C. Lin, C. Yang, Y. Shi, C. Ren, Y. Li, H. Weng, X. Dai, Z. Fang, S. Yan, and P. Xiong, Phys. Rev. Lett. **115**, 087002 (2015).
[37] Q. Liu and A. Zunger, arXiv:1611.04147.
[38] W.-J. Chen, M. Xiao, and C. T. Chan, Nat. Commun. **7**, 13038 (2016).
[39] M.-L. Chang, M. Xiao, W.-J. Chen, and C. T. Chan, arXiv:1607.02918.
[40] H.-H. Lai, Phys. Rev. B **91**, 235131 (2015).
[41] S.-K. Jian and H. Yao, Phys. Rev. B **92**, 045121 (2015).
[42] S.-X. Zhang, S.-K. Jian, and H. Yao, arXiv:1610.08975v2.
[43] S.-K. Jian and H. Yao, arXiv:1609.06313v2.
[44] B. Roy and J. D. Sau, Phys. Rev. B **92**, 125141 (2015).
[45] S. Bera, J. D. Sau, and B. Roy, Phys. Rev. B **93**, 201302(R) (2016).
[46] X. Li, B. Roy, and S. Das Sarma, Phys. Rev. B **94**, 195144 (2016).
[47] B. Roy, P. Goswami, and V. Juričić, arXiv:1610.05762v1.
[48] B. Roy, R.-J. Slager, and V. Juričić, arXiv:1610.08973v1.
[49] S. Ahn, E. H. Hwang, and H. Min, Sci. Rep. **6**, 34023 (2016).
[50] S. Ahn, E. J. Mele, and H. Min, arXiv:1609.08566v1.
[51] P. Goswami and A. H. Nevidomskyy, Phys. Rev. B **92**, 214504 (2015).
[52] H. Shapourian and T. L. Hughes, Phys. Rev. B **93**, 075108 (2016).
[53] B. Sbierski, M. Trescher, E. J. Bergholtz, and P. W. Brouwer, arXiv:1606.06941v1.
[54] L. Lepori, I. C. Fulga, A. Trombettoni, and M. Burrello, arXiv:1603.02292v1.
[55] Q. Chen and G. A. Fiete, Phys. Rev. B **93**, 155125 (2016).
[56] X. Dai, H.-Z. Lu, S.-Q. Shen, and H. Yao, Phys. Rev. B **93**, 16110(R) (2016).
[57] L.-J. Zhai, P.-H. Chou, and C.-Y. Mou, Phys. Rev. B **94**, 125135 (2016).
[58] A. Gupta, arXiv:1610.07848v1.
[59] J. Polchinski, arXiv:9210046v2.
[60] R. Shankar, Rev. Mod. Phys. **66**, 129 (1994).
[61] H. Isobe, B.-J. Yang, A. Chubukov, J. Schmalian, and N. Nagaosa, Phys. Rev. Lett. **116**, 076803 (2016).
[62] J.-R. Wang, G.-Z. Liu, and C.-J. Zhang, arXiv:1611.00145.
[63] J. González, F. Guinea, and M. A. H. Vozmediano, Nucl. Phys. B **424**, 595 (1994).
[64] D. T. Son, Phys. Rev. B **75**, 235423 (2007).
[65] C. Bauer, A. Rückriegel, A. Sharma, and P. Kopietz, Phys. Rev. B **92**, 121409(R) (2015).
[66] A. Sharma and P. Kopietz, Phys. Rev. B **93**, 235425 (2016).
[67] O. Vafek, Phys. Rev. Lett. **98**, 216401 (2007).
[68] D. E. Scheehy and J. Schmalian, Phys. Rev. Lett. **99**, 226803 (2007).
[69] A. Sekine, T. Z. Nakano, Y. Araki, and K. Nomura, Phys. Rev. B **87**, 165142 (2013).
[70] M. Sitte, A. Rosch, and L. Fritz, Phys. Rev. B **88**, 205107 (2013).
[71] P. Goswami and S. Chakravarty, Phys. Rev. Lett. **107**, 196803 (2011).
[72] P. Hosur, S. A. Parameswaran, and A. Vishwanath, Phys. Rev. Lett. **108**, 046602 (2012).
[73] J. González, Phys. Rev. B **90**, 121107(R) (2014).
[74] J. Hofmann, E. Barnes, and S. Das Sarma, Phys. Rev. B **92**, 045104 (2015).
[75] R. E. Throckmorton, J. Hofmann, E. Barnes, and S. Das Sarma, Phys. Rev. B **92**, 115101 (2015).
[76] B.-J. Yang, E.-G. Moon, H. Isobe, and N. Nagaosa, Nat. Phys. **10**, 774 (2014).
[77] A. A. Abrikosov, J. Low. Temp. Phys. **8**, 315 (1972).
[78] A. A. Abrikosov and S. D. Beneslavskii, Sov. Phys. JETP **32**, 699 (1971).
[79] A. A. Abrikosov, Sov. Phys. JETP **39**, 709 (1974).
[80] E.-G. Moon, C. Xu, Y. B. Kim, and L. Balents, Phys. Rev. Lett. **111**, 206401 (2013).
[81] I. F. Herbut and L. Janssen, Phys. Rev. Lett. **113**, 106401 (2014).
[82] L. Janssen and I. F. Herbut, Phys. Rev. B **92**, 045117 (2015).
[83] P. T. Dumitrescu, Phys. Rev. B **92**, 121102(R) (2015).
[84] L. Janssen and I. F. Herbut, Phys. Rev. B **93**, 165109 (2016).
[85] L. Janssen and I. F. Herbut, arXiv:1611.04594v1.
[86] Y. Huh, E.-G. Moon, and Y. B. Kim, Phys. Rev. B **93**, 035138 (2016).
[87] G. Y. Cho and E.-G. Moon, Sci. Rep. **6**, 19198 (2016).
[88] H. Isobe and L. Fu, Phys. Rev. B **93**, 241113 (2016).
[89] D. C. Elias, R. V. Gorbachev, A. S. Mayorov, S. V. Morozov, A. A. Zhukov, P. Blake, L. A. Ponomarenko, I. V. Grigorieva, K. S. Novoselov, F. Guinea, and A. K. Geim, Nat. Phys. **7**, 701 (2011).
[90] D. A. Siegel, C.-H. Park, C. Hwang, J. Deslippe, A. V. Fedorov, S. G. Louie, and A. Lanzara, Proc. Natl. Acad. Sci. U.S.A. **108**, 11365 (2011).
[91] G. L. Yu, R. Jalil, B. Belle, A. S. Mayorov, P. Blake, F. Schedin, S. V. Morozov, L. A. Ponomarenko, F. Chiappini, S. Wiedmann, U. Zeitler, M. I. Katsnelson, A. K. Geim, K. S. Novoselov, and D. C. Elias, Proc. Natl. Acad. Sci. U.S.A. **110**, 3282 (2013).
[92] L. Miao, Z. F. Wang, W. Ming, M.-Y. Yao, M. Wang, F. Yang, Y. R. Song, F. Zhu, A. V. Fedorov, Z. Sun, C. L. Gao, C. Liu, Q.-X. Xue, C.-X. Liu, F. Liu, D. Qian, and J.-F. Jia, Proc. Natl. Acad, Sci. U.S.A. **110**, 2758 (2013).
[93] T. Kondo, M. Nakayama, R. Chen, J. J. Ishikawa, E.-G.

Moon, T. Yamamoto, Y. Ota, W. Malaeb, H. Kanai, Y. Nakashima, Y. Ishida, R. Yoshida, H. Yamamoto, M. Matsunami, S. Kimura, N. Inami, K. Ono, H. Kumigashira, S. Nakatsuji, L. Baltents, and S. Shin, Nat. Commun. **6**, 10042 (2015).

[94] A. Damascelli, Z. Hussain, and Z.-X. Shen, Rev. Mod. Phys. **75**, 473 (2003),

[95] M. Hashimoto, I. M. Vishik, R.-H. He, T. P. Devereaux, and Z.-X. Shen, Nat. Phys. **10**, 483 (2014).

[96] J.-R. Wang, G.-Z. Liu, and C.-J. Zhang. New J. Phys. **18**, 073023 (2016).